Image Reconstruction

Marc Kachelrieß

German Cancer Research Center (DKFZ)
Heidelberg, Germany
www.dkfz.de/ct

DEUTSCHES
KREBSFORSCHUNGSZENTRUM
IN DER HELMHOLTZ-GEMEINSCHAFT

Contents

- Analytical Image Reconstruction (90 min)
  - Filtered backprojection
  - Gridding
  - Applications in CT, MR, PET, SPECT, ...
- Iterative image Reconstruction (90 min)
  - Kaczmarz, PWLS
  - Statistical reconstruction
  - Applications in CT, MR, PET, SPECT, ...

Not Contained

- Preprocessing
- Postprocessing
- Artifact correction
- …

Fan-Beam Geometry (transaxial / in-plane / x-y-plane)

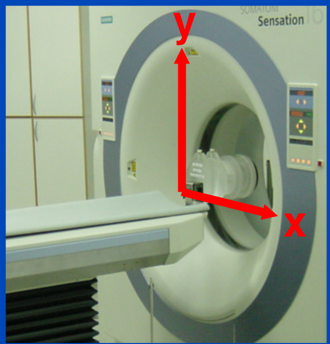

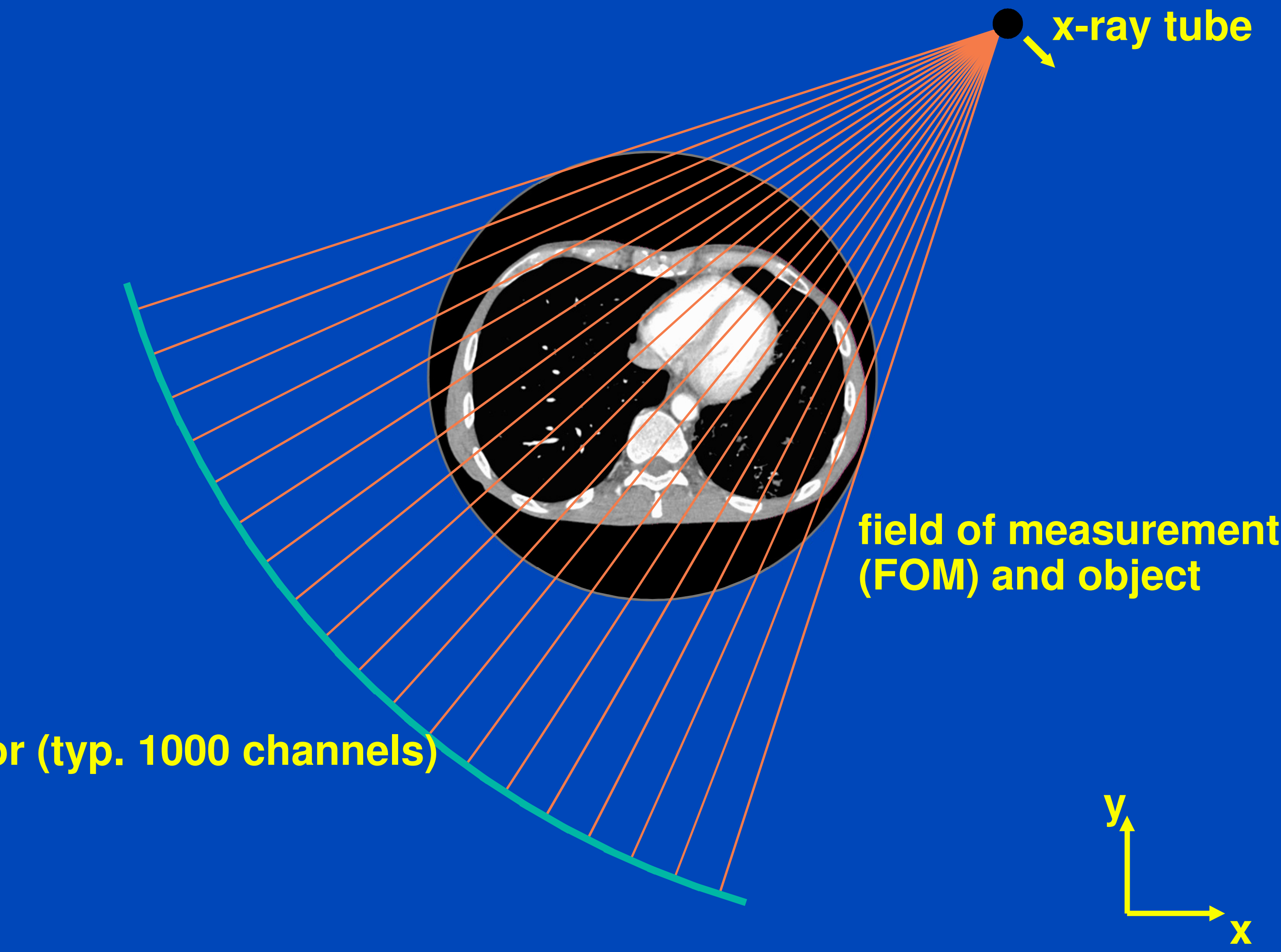

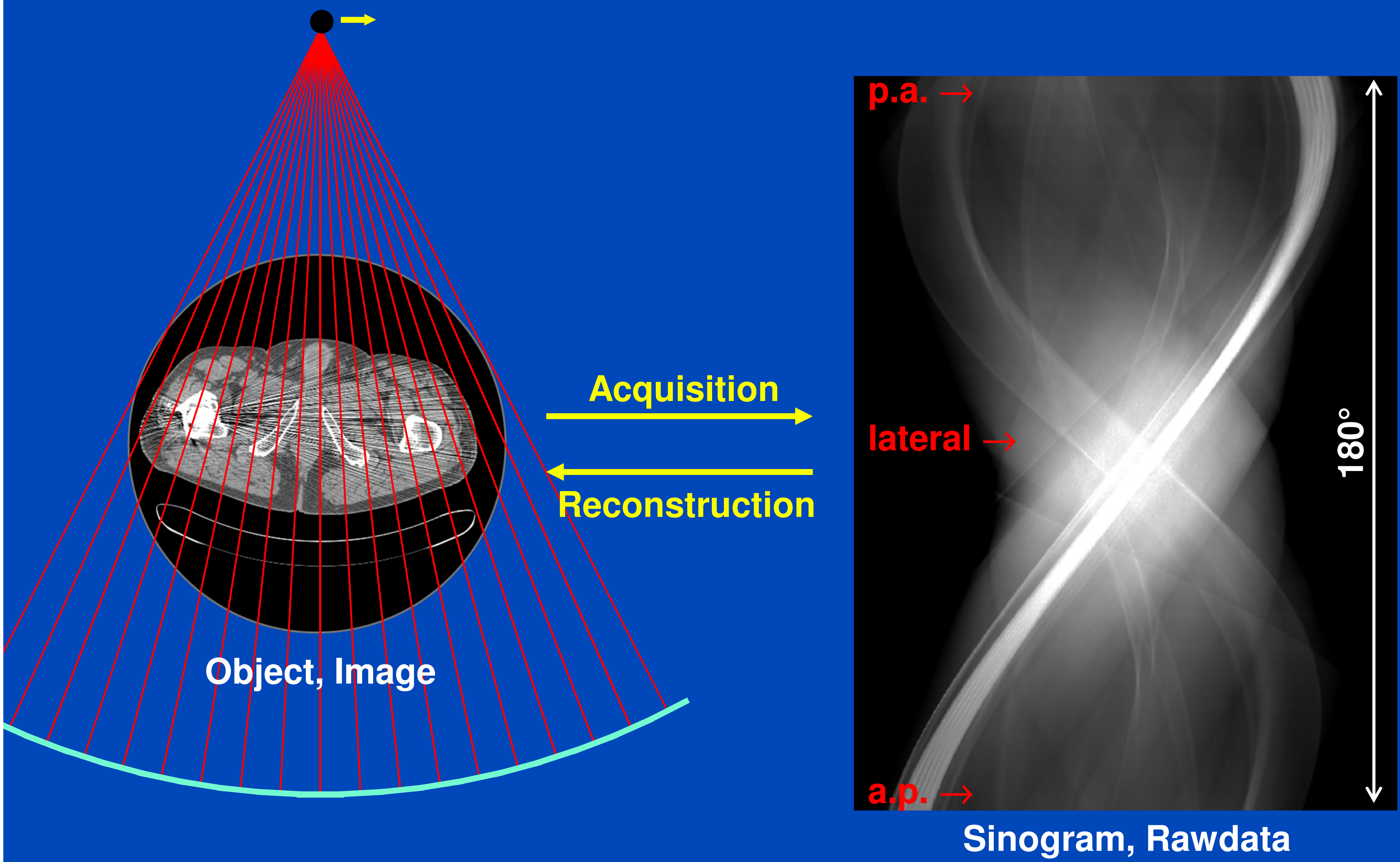

Acquisition
Reconstruction
Object, Image
p.a. →
lateral →
a.p. →
180°
Sinogram, Rawdata

dkfz.

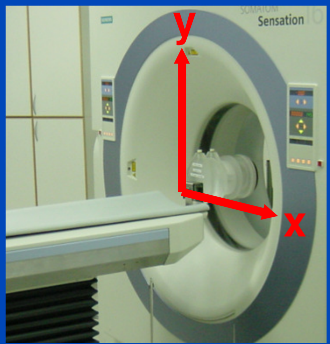

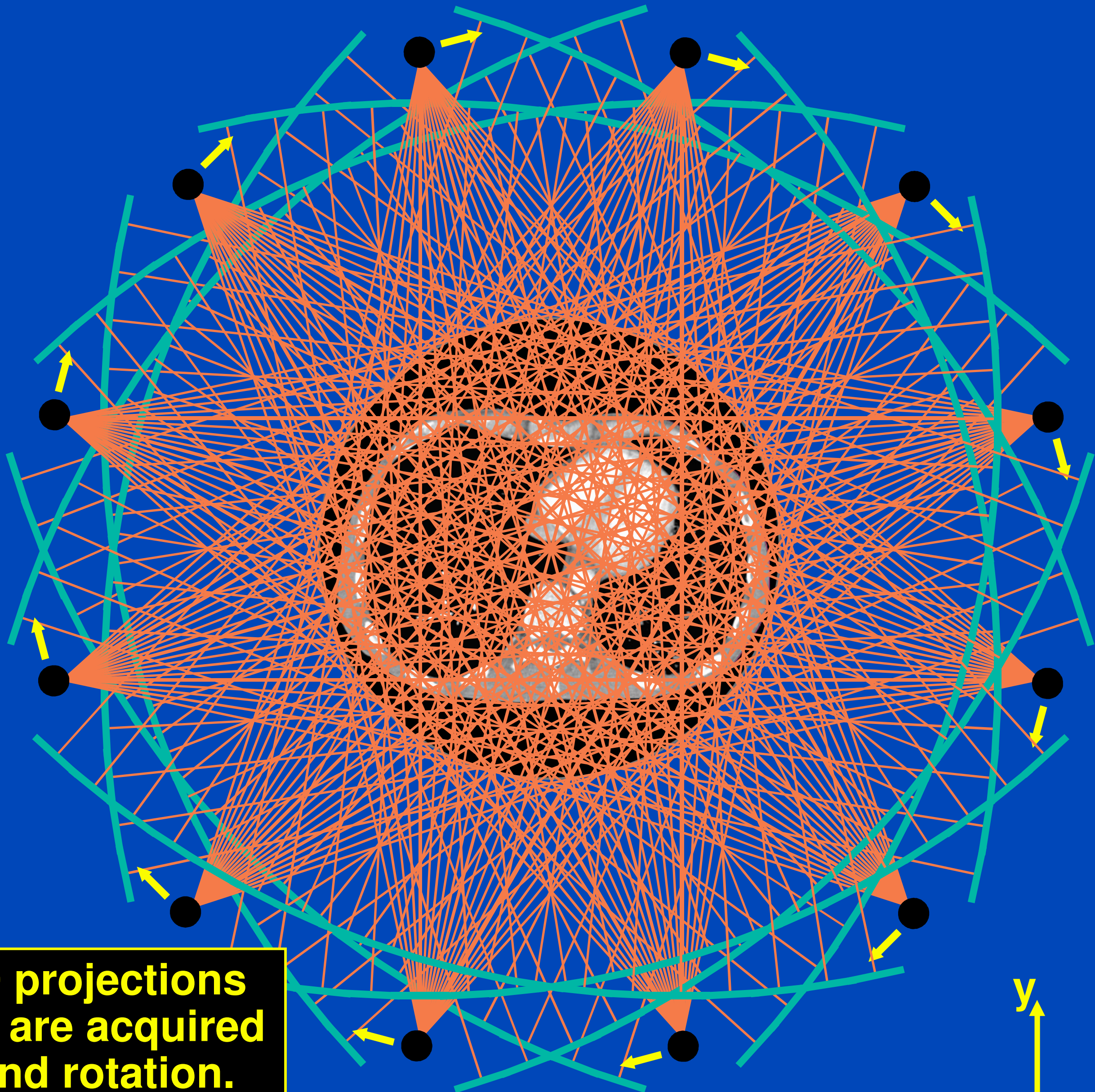

In the order of 1000 projections with 1000 channels are acquired per detector slice and rotation.

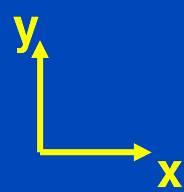

Data Completeness

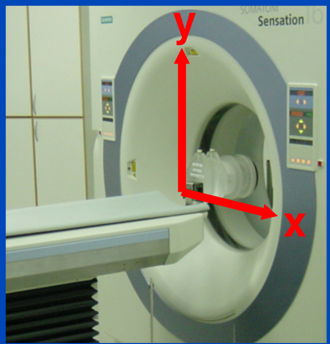

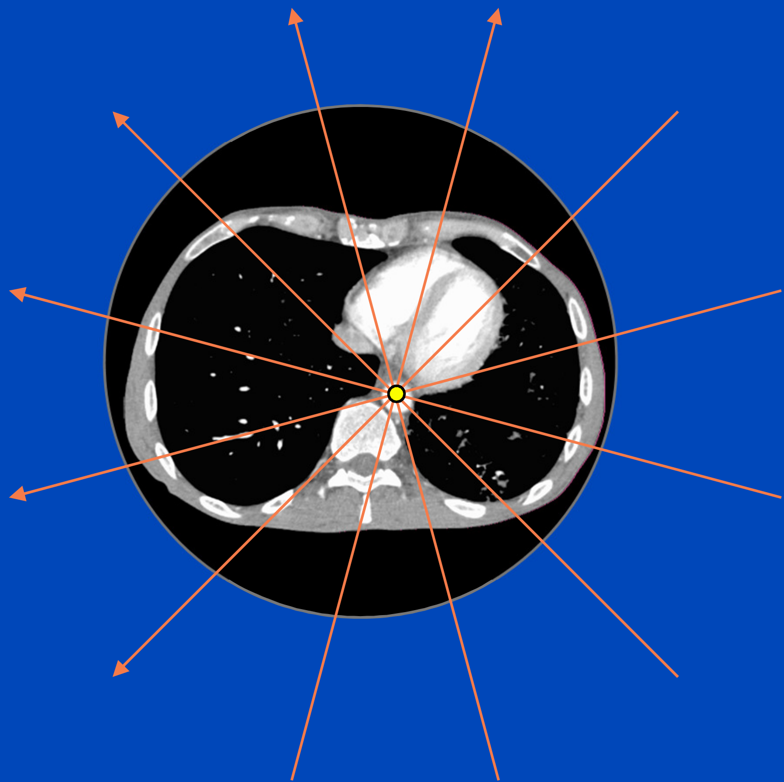

Each object point must be viewed by an angular interval of 180° or more. Otherwise image reconstruction is not possible.

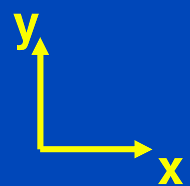

Data Completeness

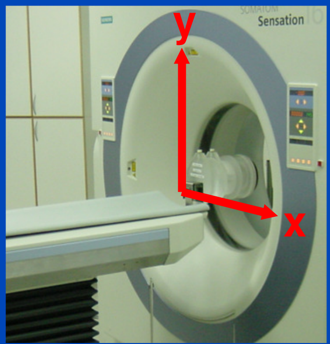

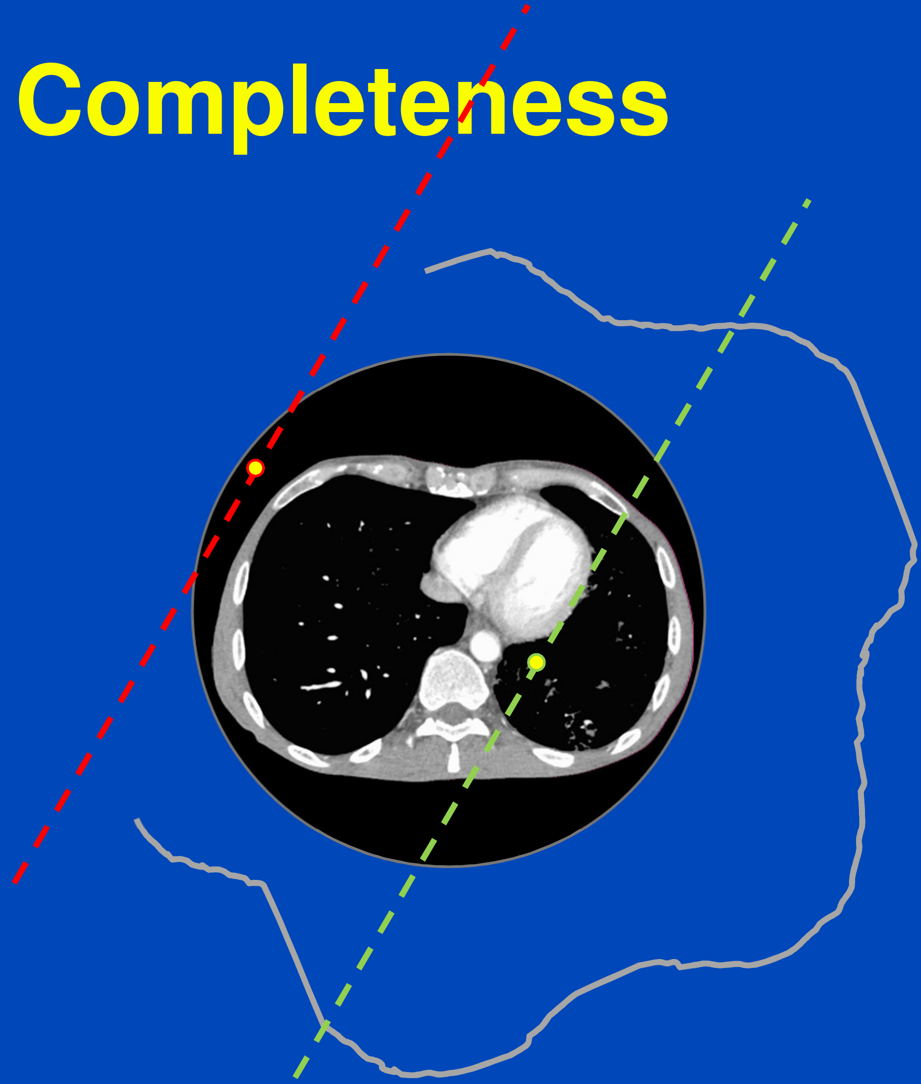

Any straight line through a voxel must be intersected by the source trajectory at least once.

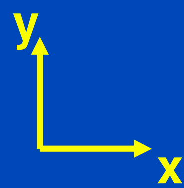

Emission vs. Transmission

Emission tomography

- Infinitely many sources
- No source trajectory
- Detector trajectory may be an issue
- 3D reconstruction relatively simple

Transmission tomography

- A single source
- Source trajectory is the major issue
- Detector trajectory is an important issue
- 3D reconstruction extremely difficult

Part 1

Analytical Image Reconstruction

$$x^2 = y$$

Model

$$x = \sqrt{y}$$

Solution

2D: In-Plane Geometry

- Decouples from longitudinal geometry
- Useful for many imaging tasks
- Easy to understand
- 2D reconstruction
  - Rebinning = resampling, resorting
  - Filtered backprojection

Fan-beam geometry **Parallel-beam geometry**

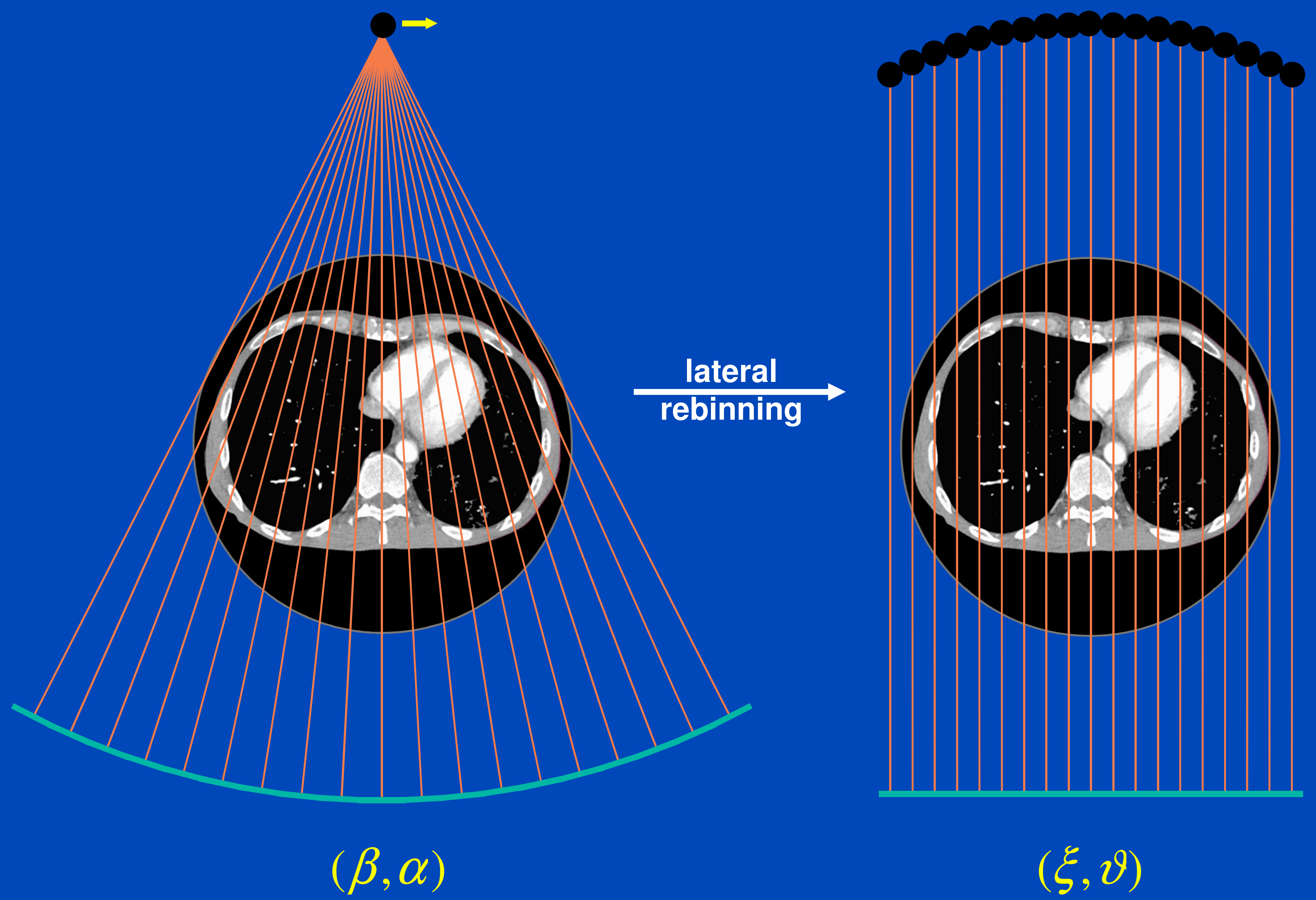

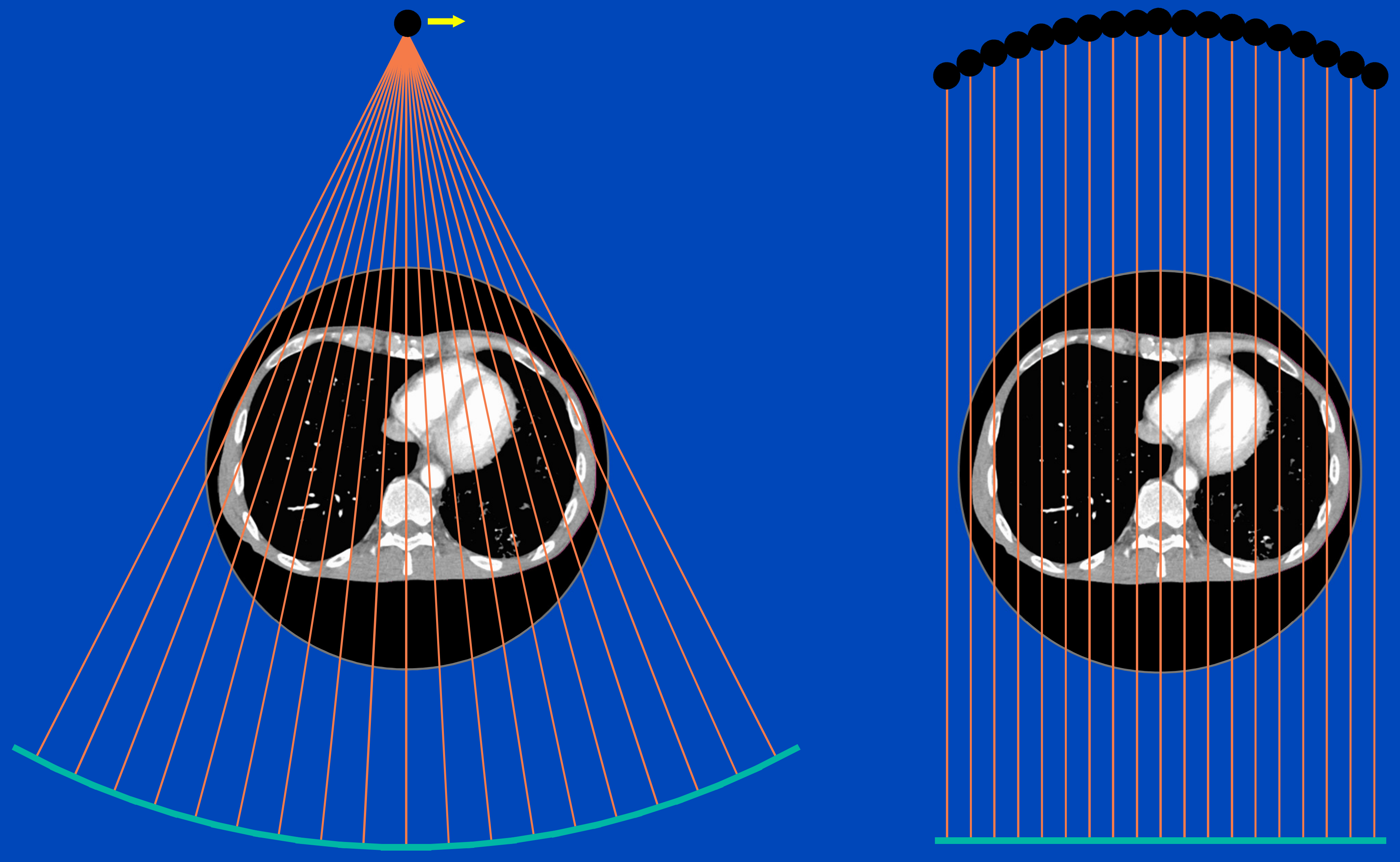

Fan-beam geometry

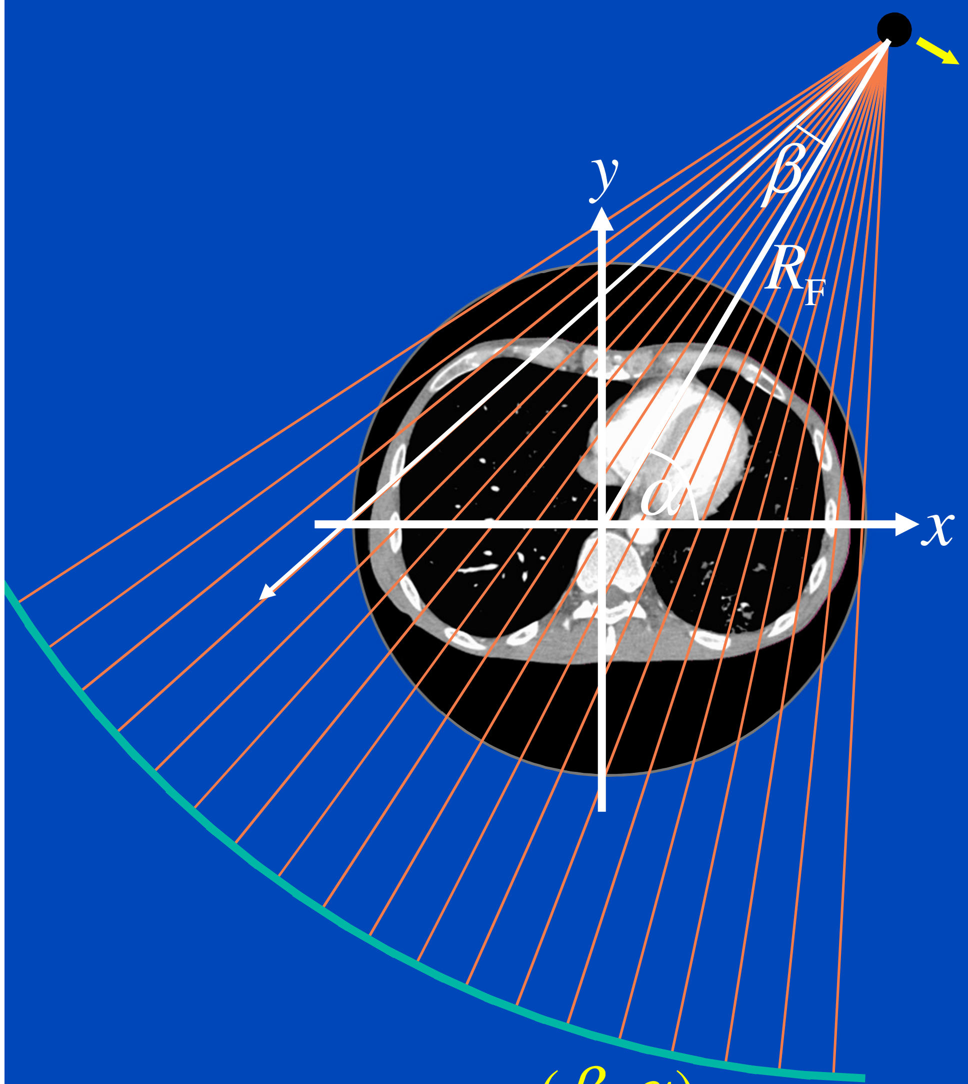

(β,α)

Parallel-beam geometry

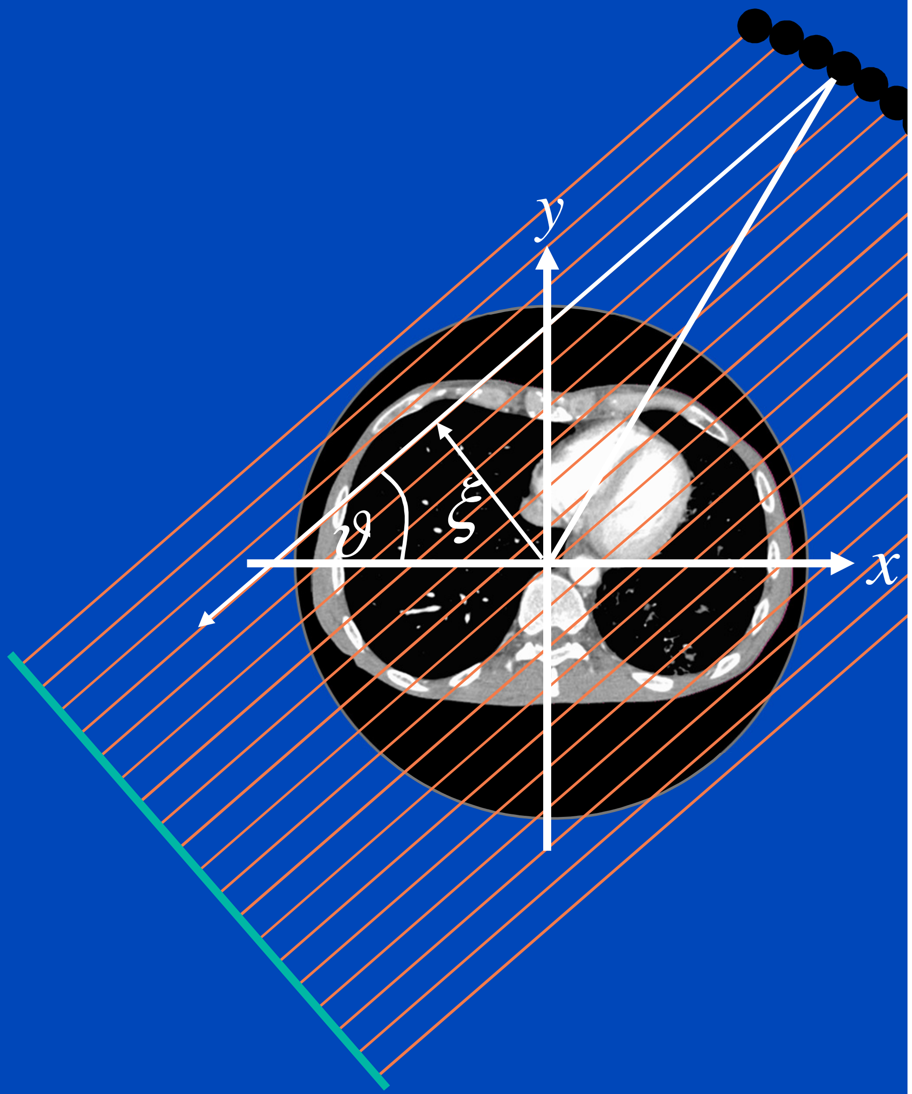

(ξ,ϑ)

In-Plane Parallel Beam Geometry

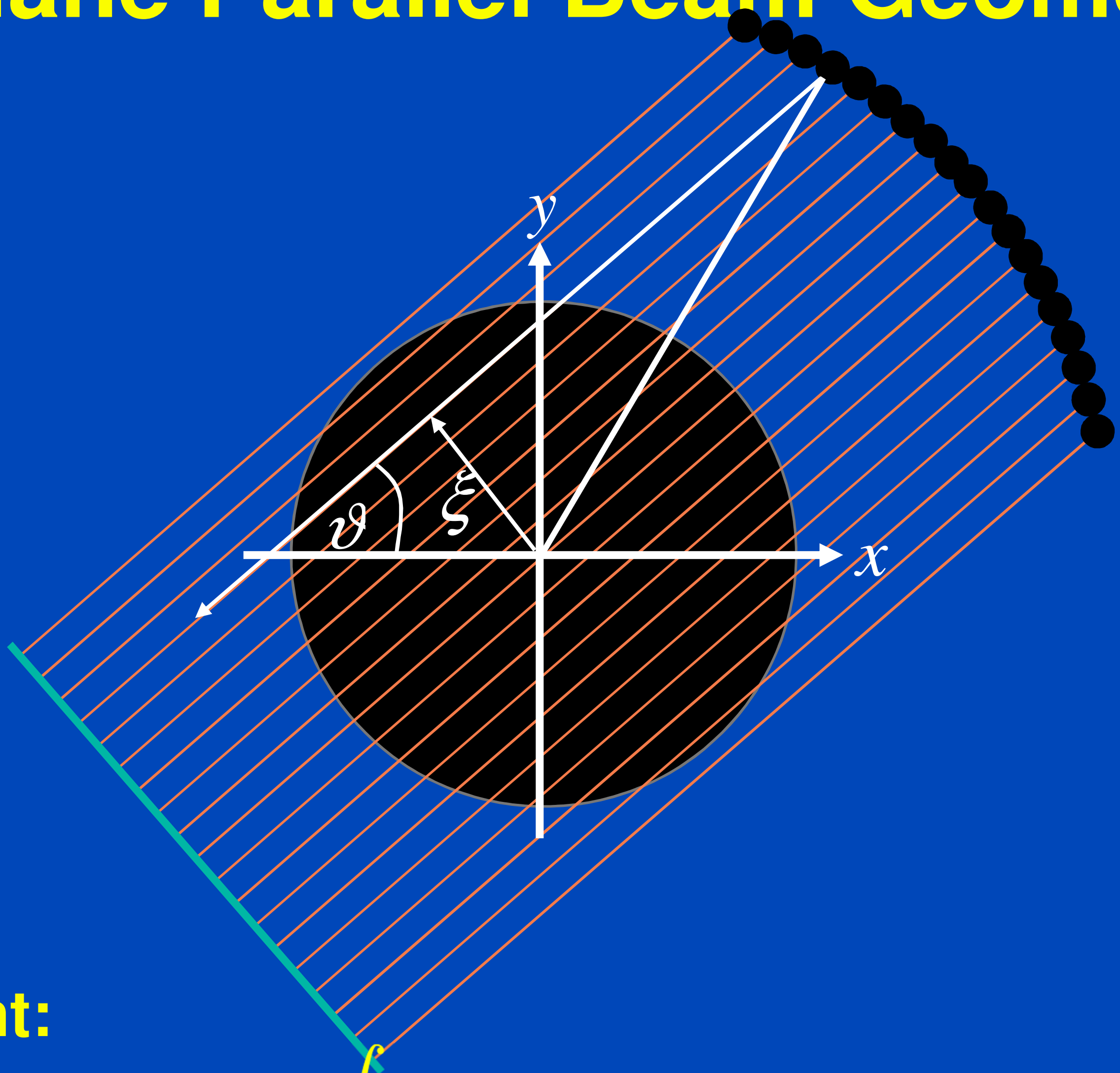

Measurement:

$$p(\vartheta,\xi) = \mathsf{X}f(\vartheta,\xi) = \int dx\,dy\, f(x,y)\,\delta(x\cos\vartheta + y\sin\vartheta - \xi)$$

Analytical Image Reconstruction
Filtered Backprojection

Filtered Backprojection (FBP)

Measurement: $p(\vartheta,\xi) = \int dxdy\, f(x,y)\delta(x\cos\vartheta + y\sin\vartheta - \xi)$

Fourier transform:

$$\int d\xi\, p(\vartheta,\xi)e^{-2\pi i\xi u} = \int dxdy\, f(x,y)e^{-2\pi i u(x\cos\vartheta + y\sin\vartheta)}$$

This is the central slice theorem: $P(\vartheta,u) = F(u\cos\vartheta, u\sin\vartheta)$

Inversion: $f(x,y) = \int\limits_0^\pi d\vartheta \int\limits_{-\infty}^{\infty} du\, |u| P(\vartheta,u)e^{2\pi i u(x\cos\vartheta + y\sin\vartheta)}$

$$= \int\limits_0^\pi d\vartheta\, p(\vartheta,\xi) * k(\xi)\Big|_{\xi = x\cos\vartheta + y\sin\vartheta}$$

Filtered Backprojection (FBP)

1. Filter projection data with the reconstruction kernel.
2. Backproject the filtered data into the image:

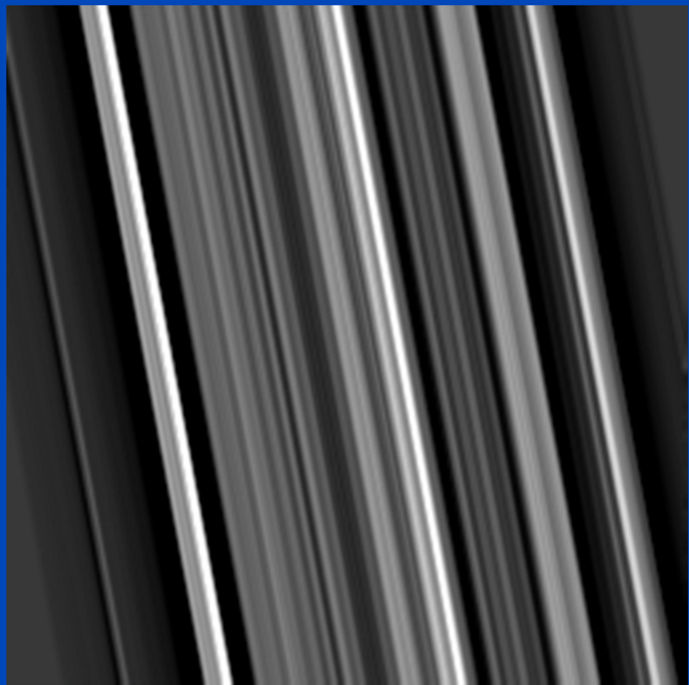

Smooth

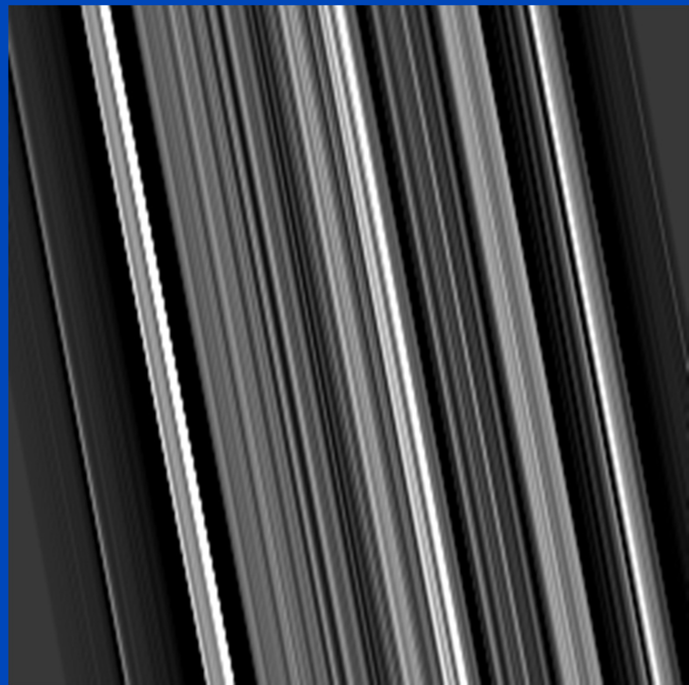

Standard

Reconstruction kernels balance between spatial resolution and image noise.

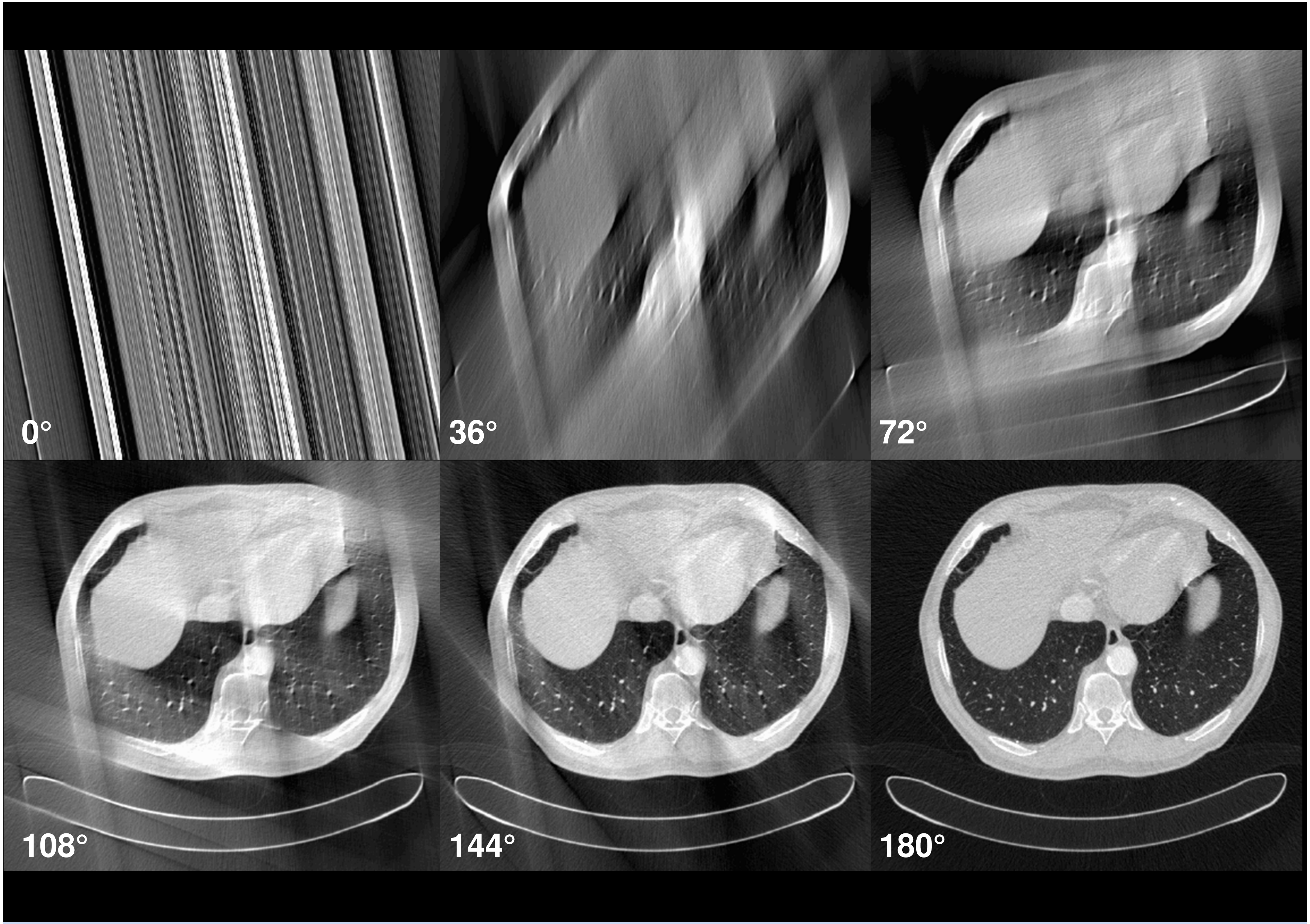

dkfz.

Backprojection
(typically destination-driven, i.e. voxel-driven)

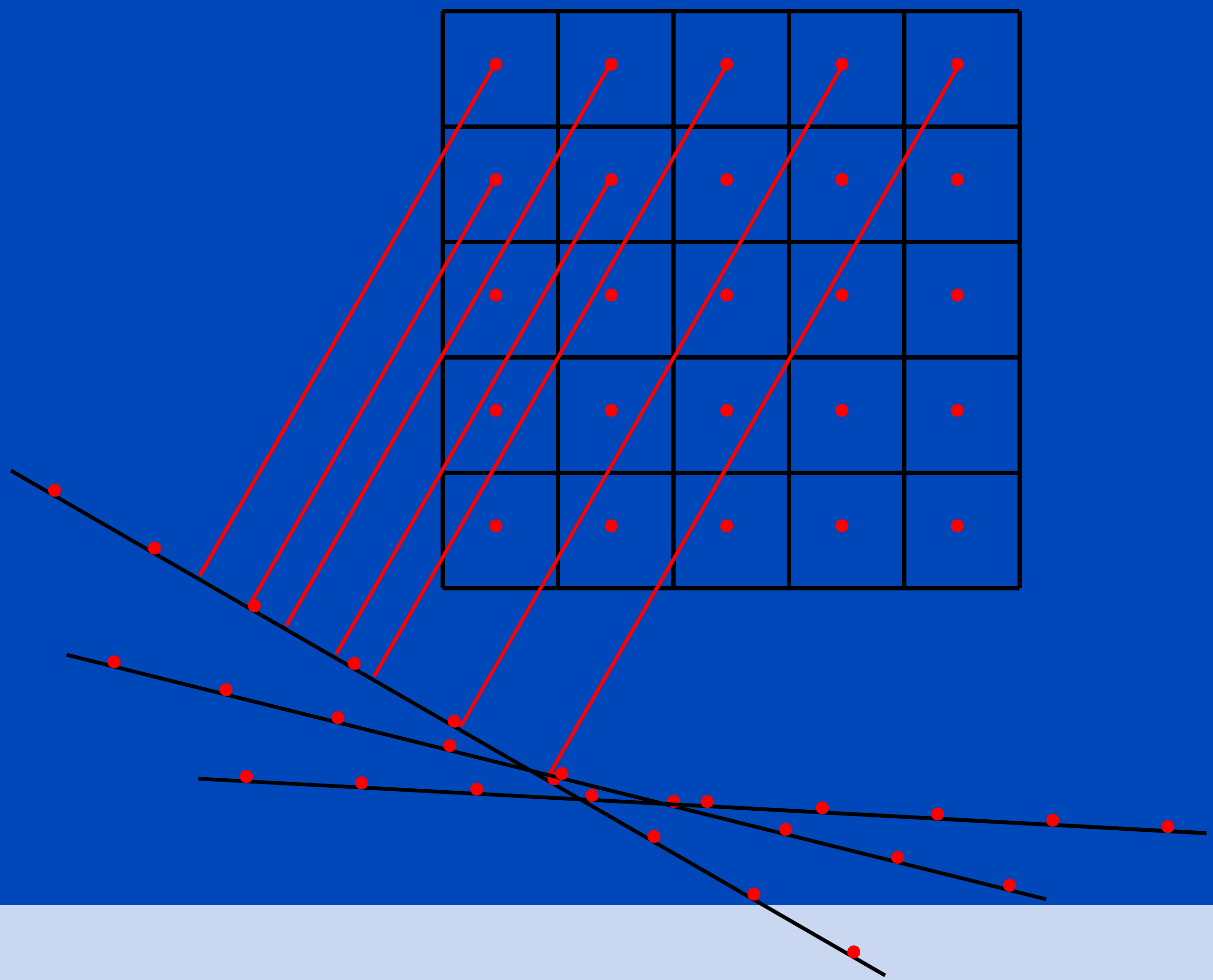

Parallel Backprojection: Reference Implementation

```
void ParBackProjRefLI(float       * const Vol, int const I, int const J, int const K,
                      float const * const Raw, int const N, int const M,
                      float const * const c0, ..., float const * const c2)
   {
   for(int n=0; n<N; n++) // projection index (theta)
   for(int i=0; i<I; i++) // slow voxel index (x)
   for(int j=0; j<J; j++) // med. voxel index (y)
      {
      float const mreal=c0[n]*i+c1[n]*j+c2[n]; // detector channel index (xi)
        int const m =int(mreal); // lower sample position
      float const wm=mreal-m; // linear interpolation weight

      for(int k=0; k<K; k++) // fast voxel and detector row index (z)
         {
         #define V(i, j, k) Vol[((i)*J+j)*K+k] // linear memory layout, use V and
         #define R(n, m, k) Raw[((n)*M+m)*K+k] // R as shortcuts for Vol and Raw

         V(i, j, k)+=(1-wm)*R(n, m, k)+wm*R(n, m+1, k);

         #undef V
         #undef R
         }
      }
   }
```

Fan-beam geometry

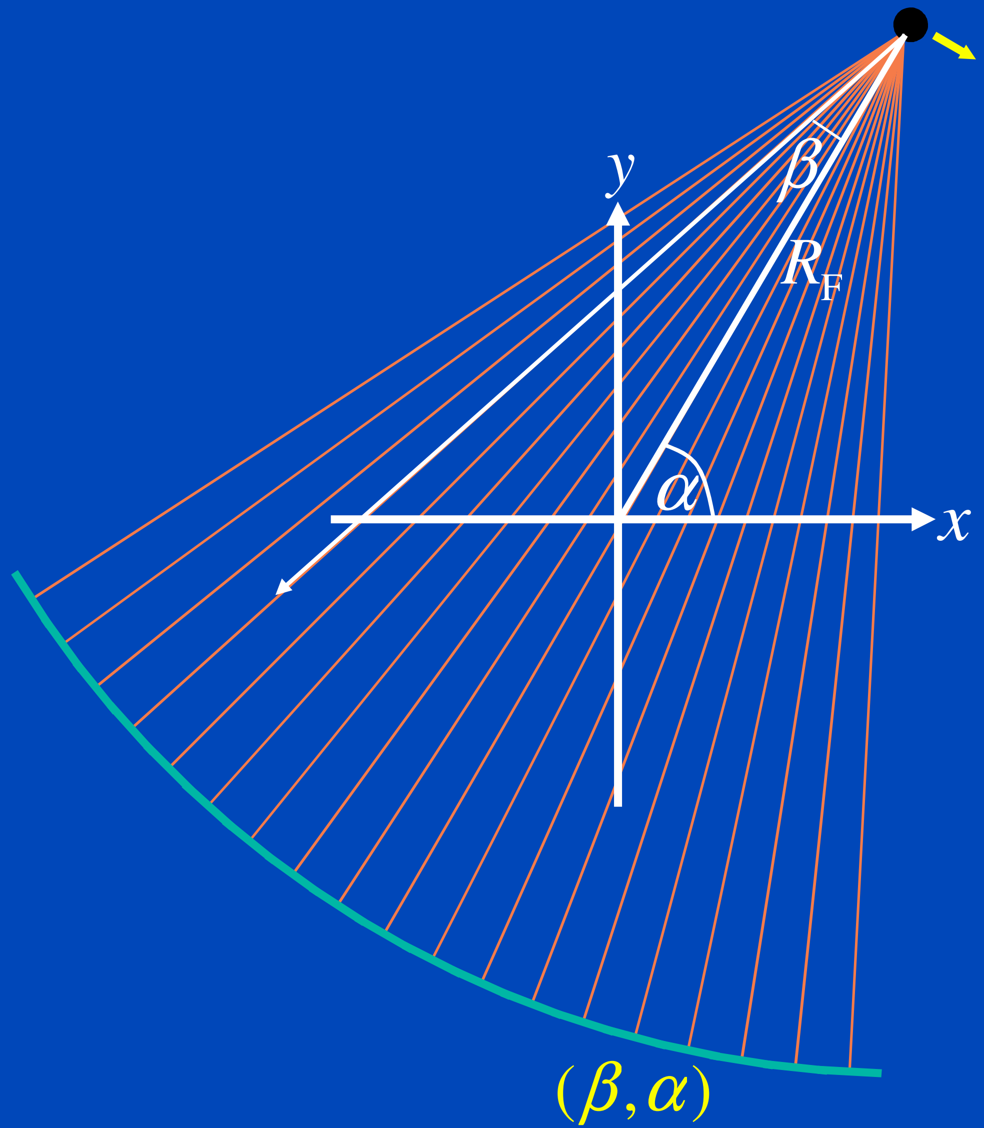

2D Fan-Beam FBP

- Some fan-beam geometries lend themselved to filtered backprojection without rebinning[1].
- Among those geometries the geometry with equiangular sampling in β, i.e. in steps of $\Delta\beta$, is the most prominent one (although not necessarily optimal).
- The second most prominent geometry that allows for filtered backprojection in the native geometry is the one corresponding to a flat detector.
- The fourth generation CT geometry does not allow for shift-invariant filtering, unless the distance R_F of the focal spot to the isocenter equals the radius R_D of the detector ring.

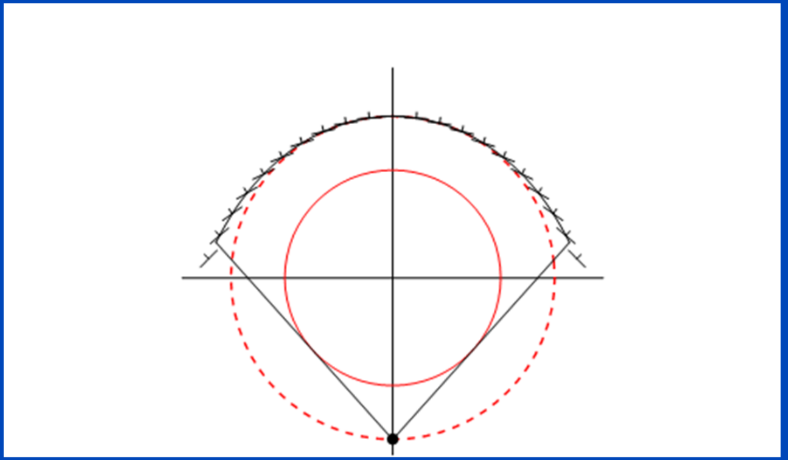

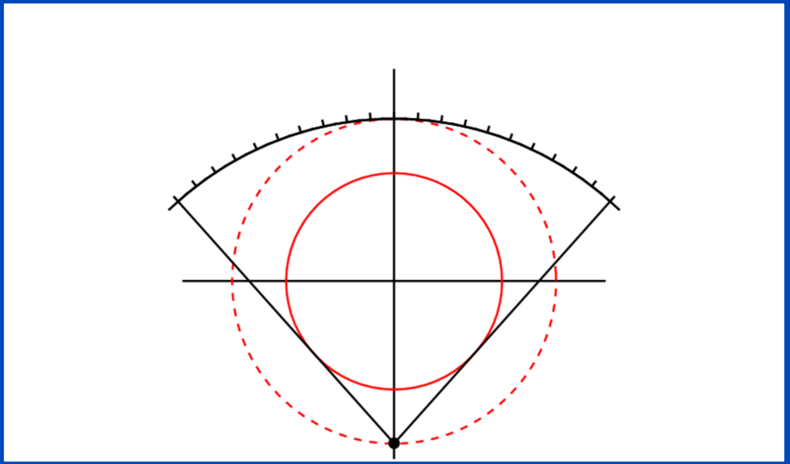

[1]Guy Besson. CT fan-beam parametrizations leading to shift-invariant filtering. Inv. Prob. 1996.

2D Fan-Beam FBP

- **Classical way (coordinate transform):**

$$f(\boldsymbol{r}) = \tfrac{1}{2}\int_0^{2\pi} d\alpha \frac{1}{|\boldsymbol{r}-\boldsymbol{s}(\alpha)|^2}\; R_{\mathrm{F}}\cos\beta\, q(\alpha,\beta) * k(\sin\beta)\Big|_{\beta=\hat\beta(\alpha,\boldsymbol{r})}$$

- **Modern way[1] (inspired by Katsevich's work):**

$$f(\boldsymbol{r}) = \tfrac{1}{2}\int_0^{2\pi} d\alpha \frac{1}{|\boldsymbol{r}-\boldsymbol{s}(\alpha)|}\; (\partial_\beta - \partial_\alpha)\, q(\alpha,\beta) * K(\sin\beta)\Big|_{\beta=\hat\beta(\alpha,\boldsymbol{r})}$$

- **Parallel beam FBP for comparison:**

$$f(\boldsymbol{r}) = \tfrac{1}{2}\int_0^{2\pi} d\vartheta\, p(\vartheta,\xi) * k(\xi)\Big|_{\xi=\hat\xi(\vartheta,\boldsymbol{r})}$$

$$\hat\beta(\alpha,\boldsymbol{r}) = -\sin^{-1}\frac{x\cos\alpha + y\sin\alpha}{|\boldsymbol{r}-\boldsymbol{s}(\alpha)|}$$

$$\hat\xi(\vartheta,\boldsymbol{r}) = x\cos\vartheta + y\sin\vartheta$$

[1]F. Noo et al. Image reconstruction from fan-beam projections on less than a short scan. PMB 2002.

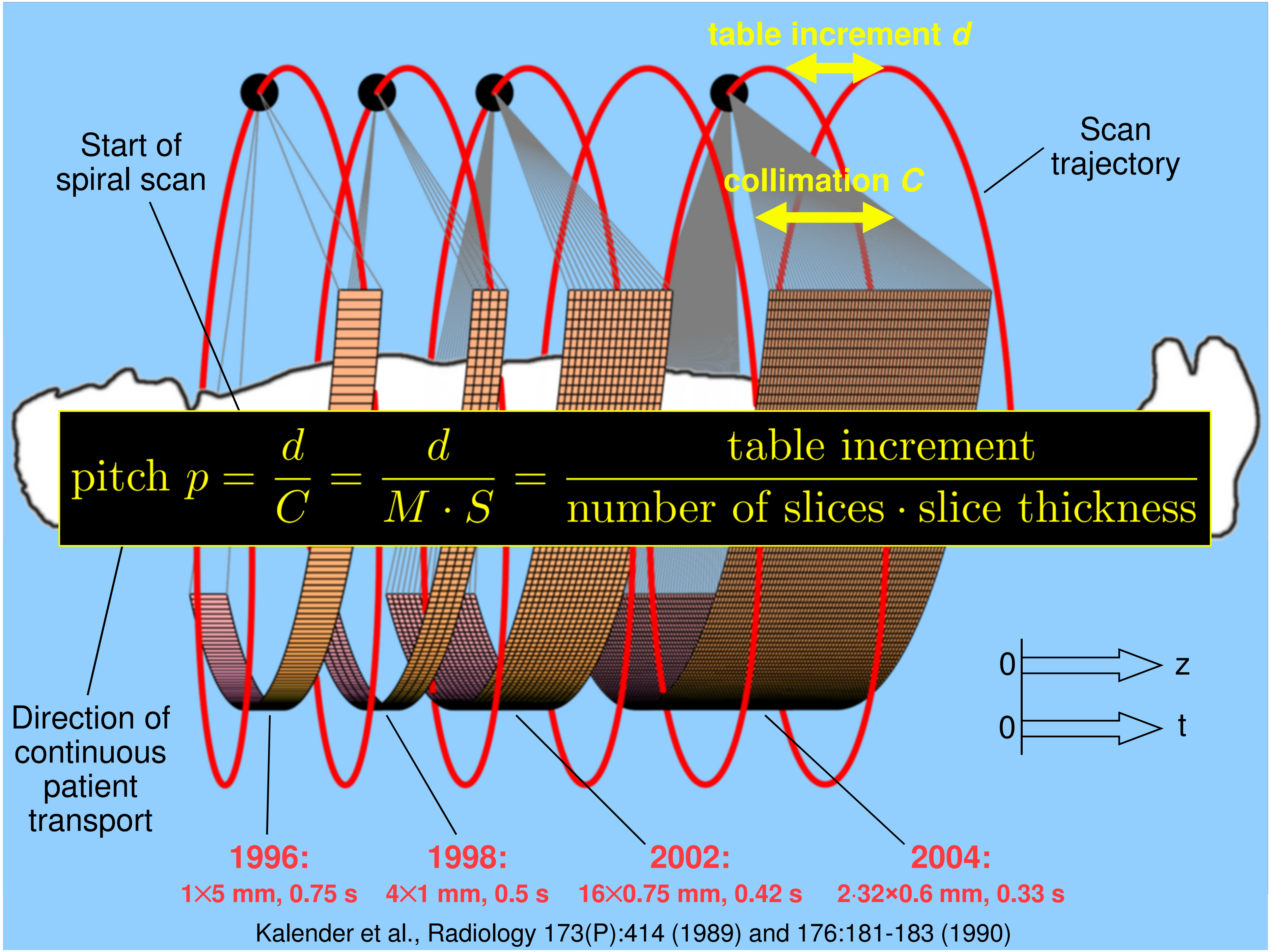

table increment d
Start of spiral scan
Scan trajectory
collimation C
$$\text{pitch } p = \frac{d}{C} = \frac{d}{M \cdot S} = \frac{\text{table increment}}{\text{number of slices} \cdot \text{slice thickness}}$$
0 z
0 t
Direction of continuous patient transport
1996:
1×5 mm, 0.75 s
1998:
4×1 mm, 0.5 s
2002:
16×0.75 mm, 0.42 s
2004:
2·32×0.6 mm, 0.33 s
Kalender et al., Radiology 173(P):414 (1989) and 176:181-183 (1990)

360° LI Spiral z-Interpolation for Single-Slice CT (M=1)

$$p = \frac{d}{MS} \le 2$$

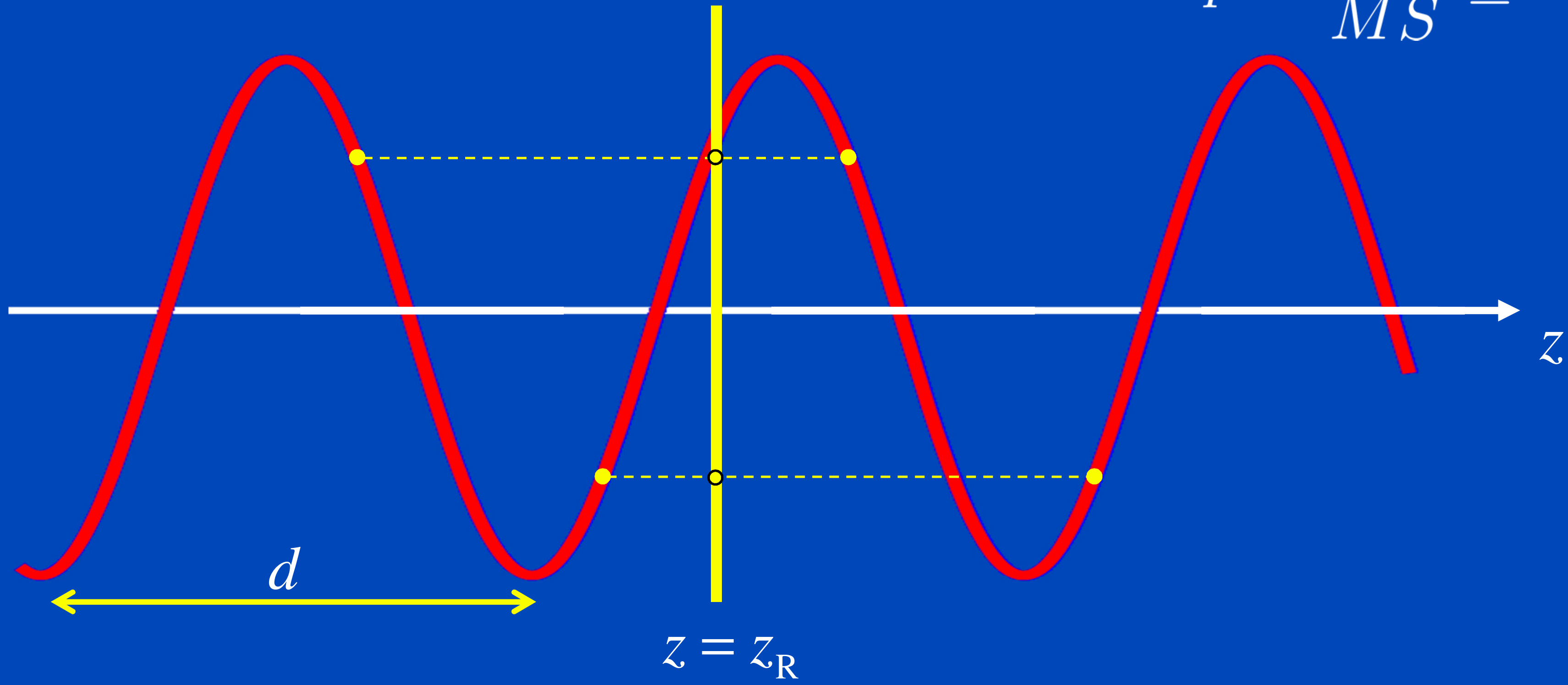

Spiral z-interpolation is typically a linear interpolation between points adjacent to the reconstruction position to obtain circular scan data.

without *z*-interpolation

with *z*-interpolation

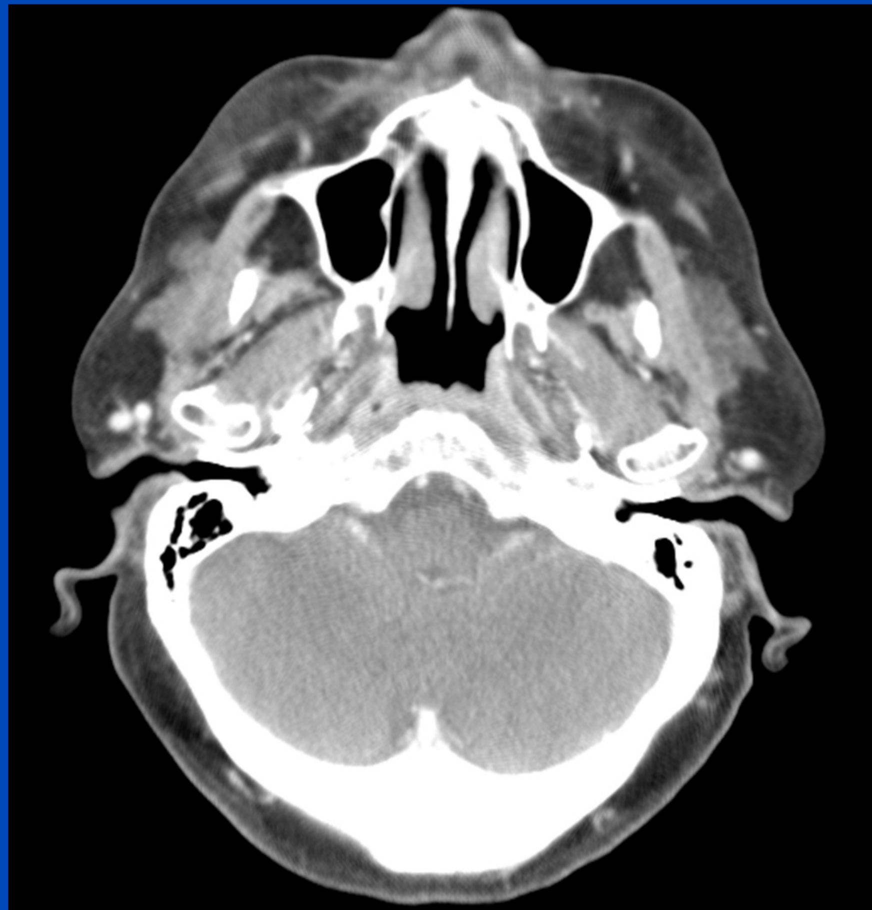

180° LI Spiral z-Interpolation for Single-Slice CT (*M*=1)

$$p = \frac{d}{MS} \leq 2$$

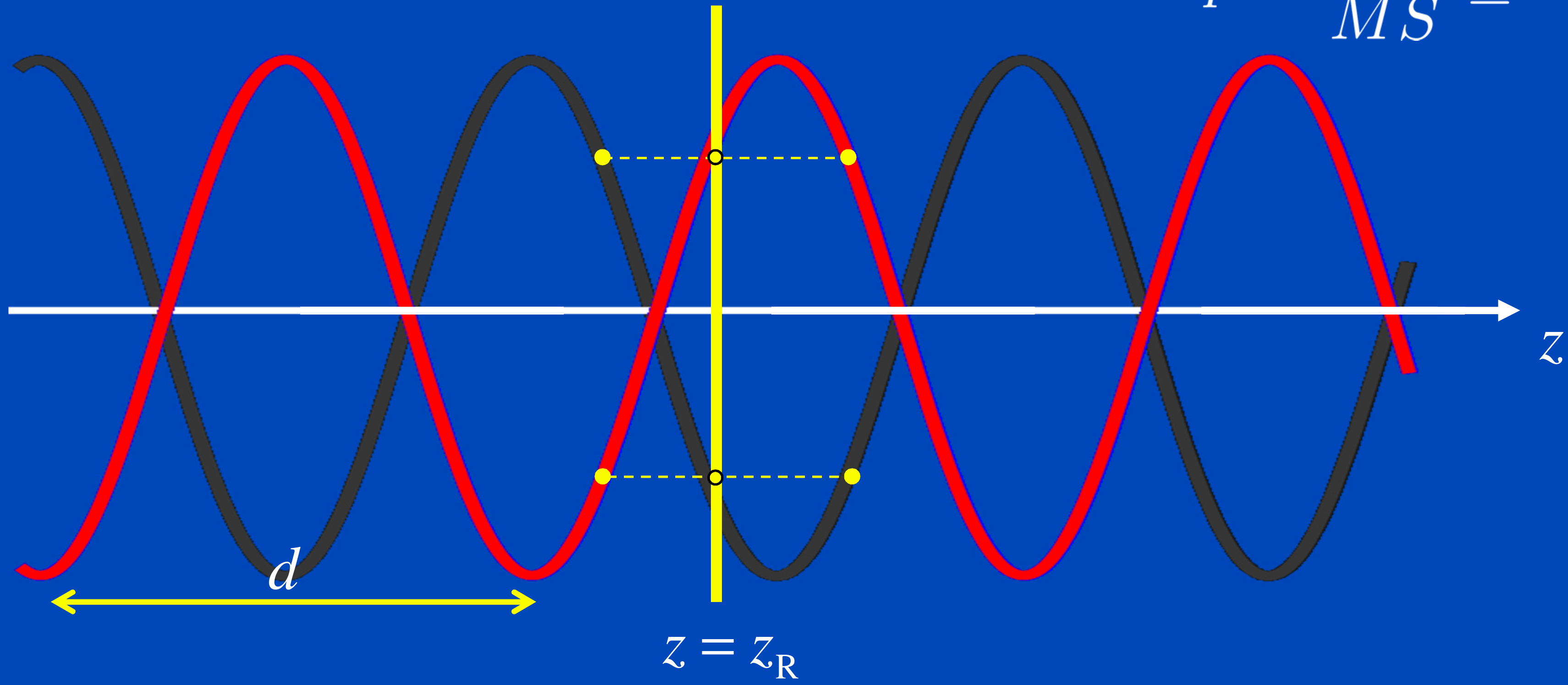

180° Spiral z-interpolation interpolates between direct and complementary rays.

dkfz.

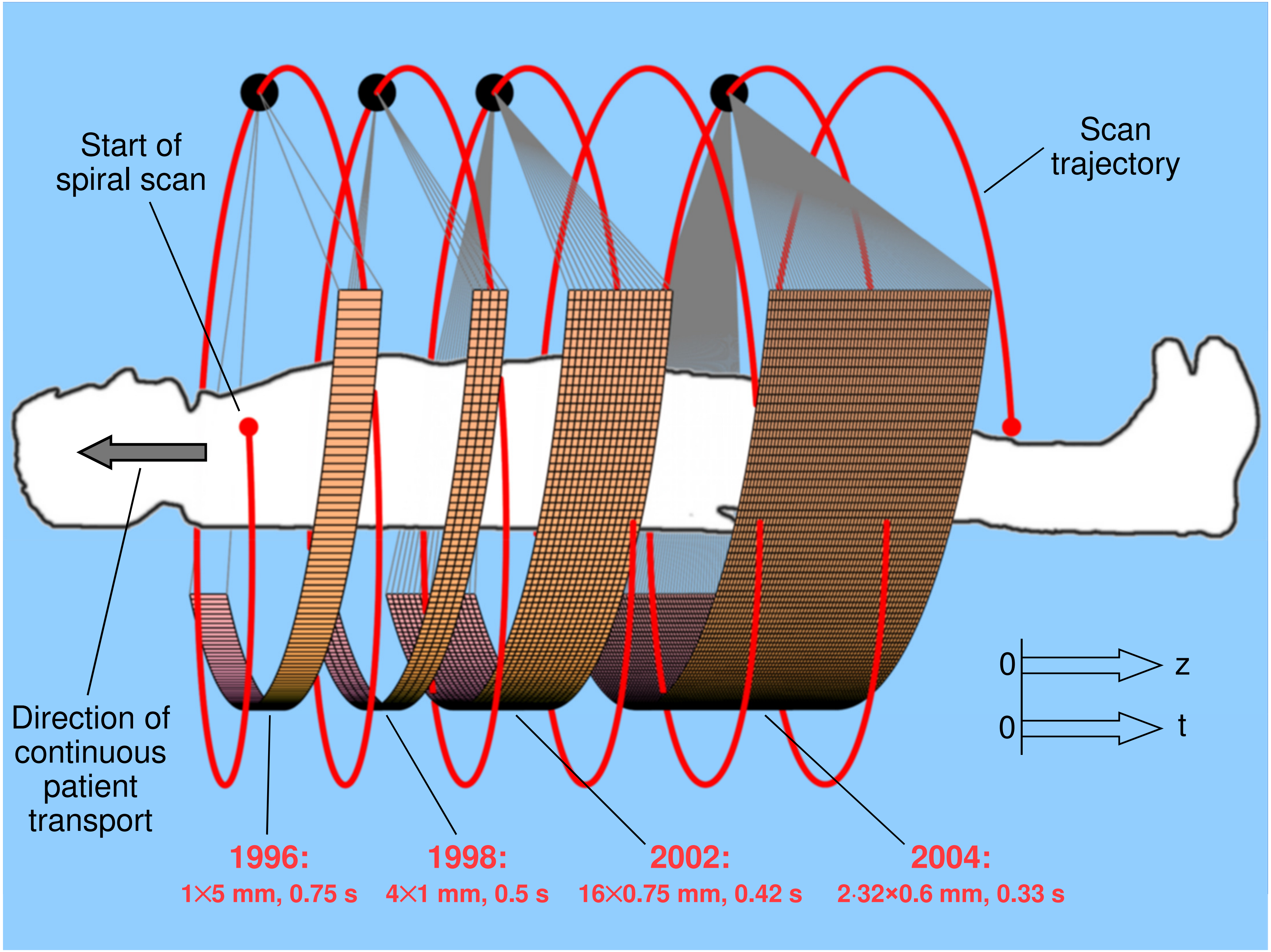
Start of
spiral scan
Scan
trajectory
Direction of
continuous
patient
transport
0 z
0 t
1996:
1×5 mm, 0.75 s
1998:
4×1 mm, 0.5 s
2002:
16×0.75 mm, 0.42 s
2004:
2·32×0.6 mm, 0.33 s

Spiral z-Filtering for Multi-Slice CT
M=2, …, 6

$$p = \frac{d}{MS} \le 1.5$$

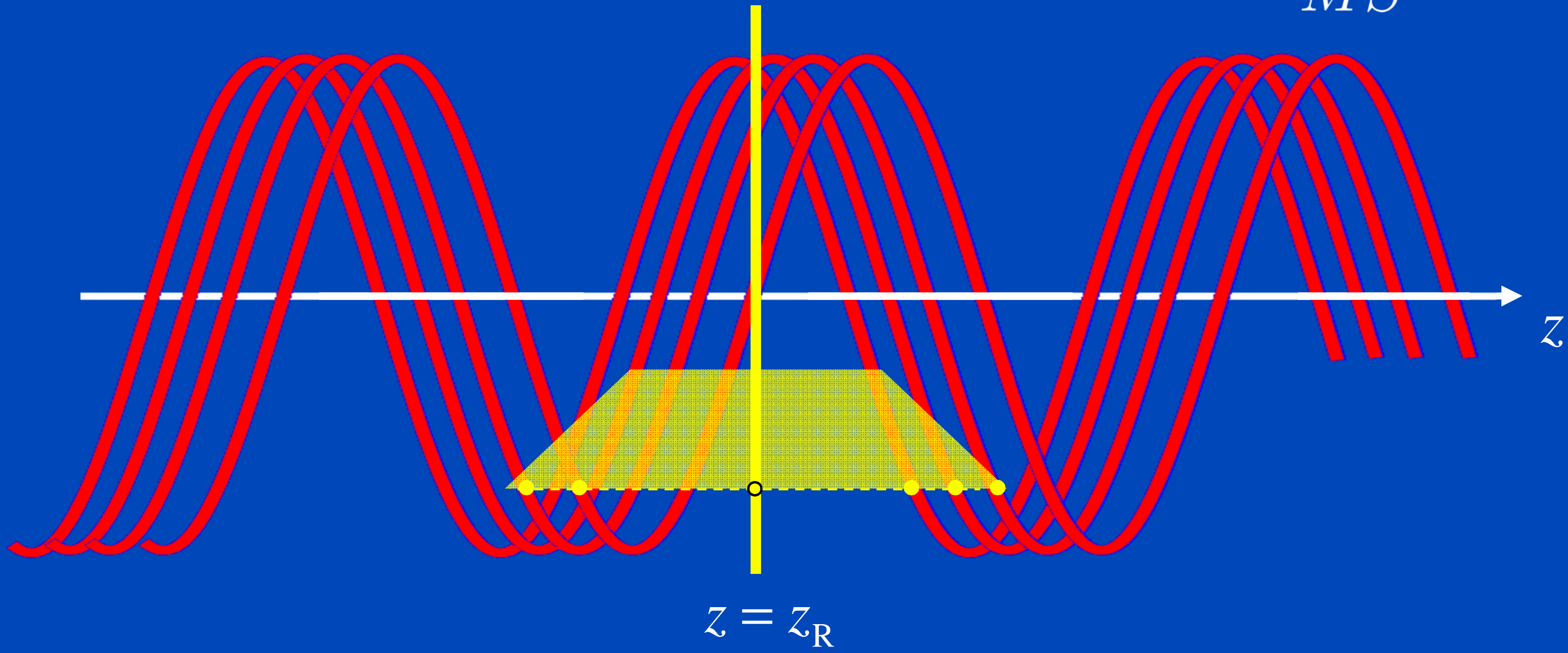

Spiral z-filtering is collecting data points weighted with a triangular or trapezoidal distance weight to obtain circular scan data.

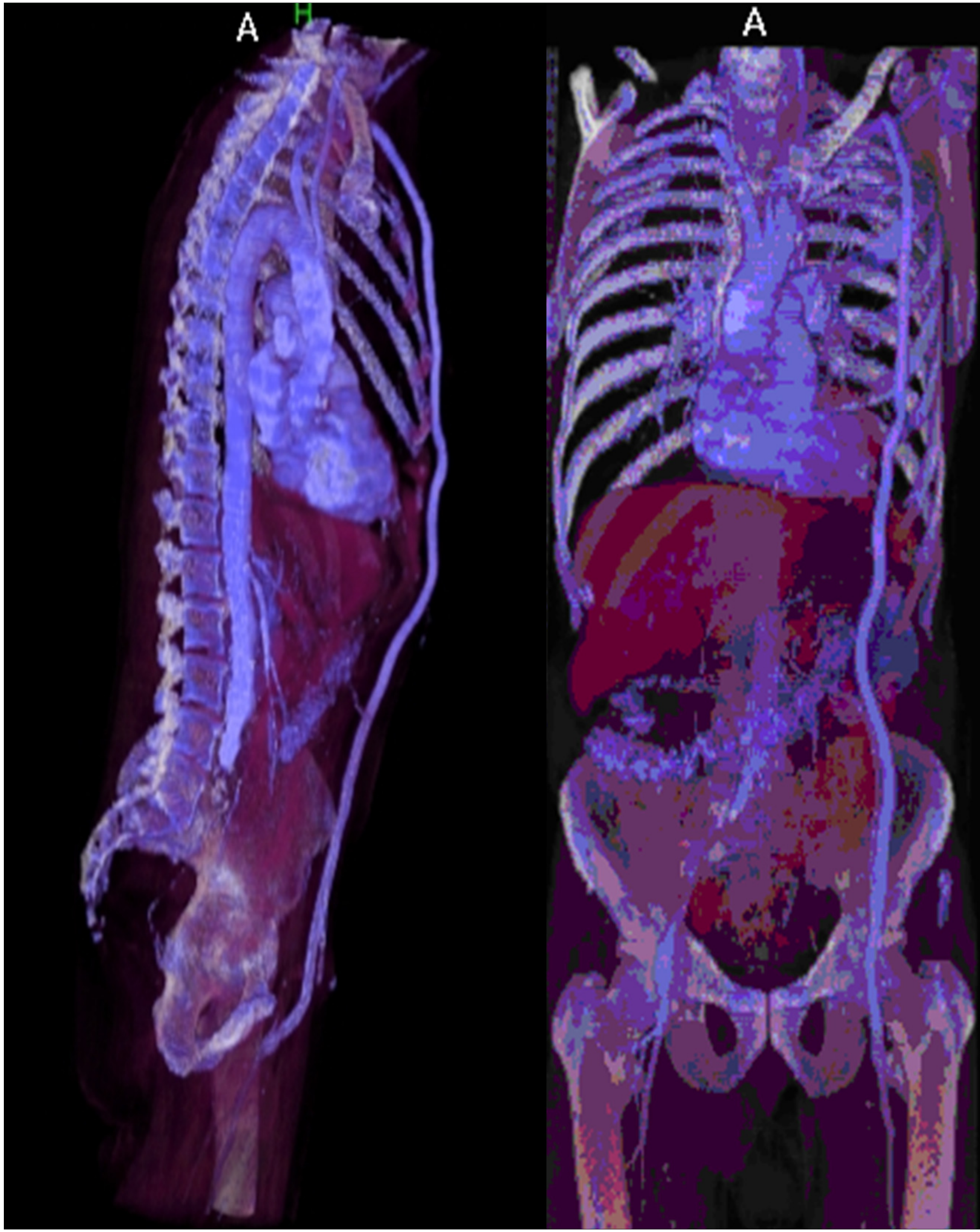

CT Angiography: Axillo-femoral bypass

M = 4

120 cm in 40 s

0.5 s per rotation
4×2.5 mm collimation
pitch 1.5

RSNA 1989
SSCT ($M = 1$)

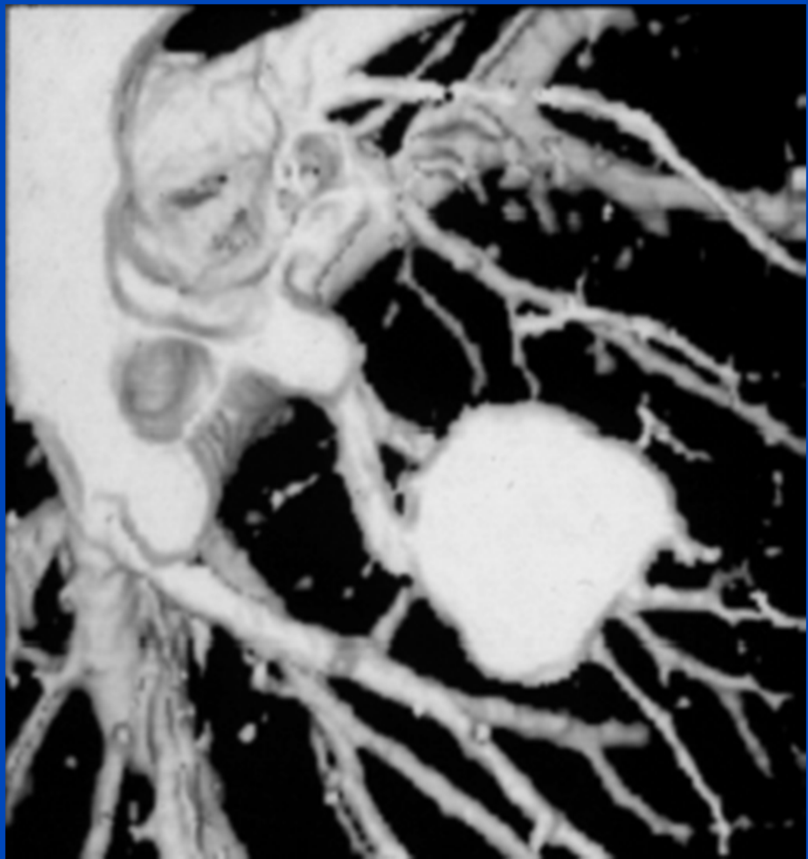

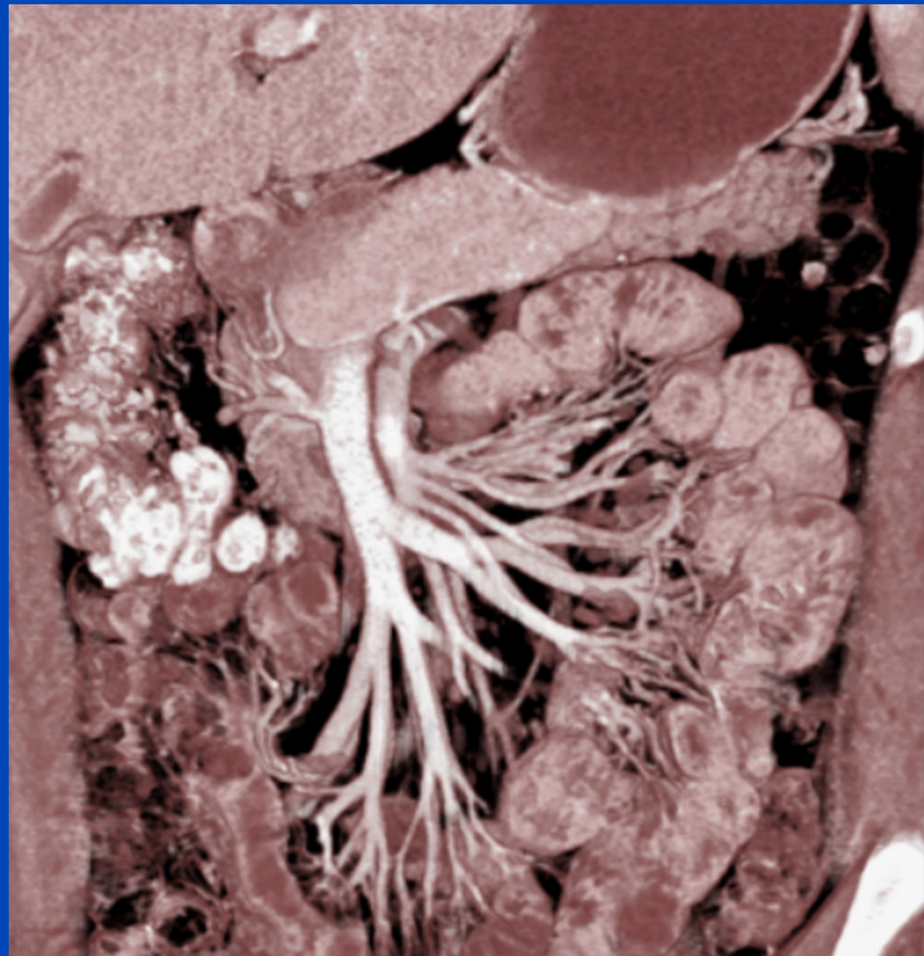

RSNA 2001
MSCT ($M = 16$)

The Pitch Value is the Measure for Scan Overlap

The pitch is defined as the ratio of the table increment per full rotation to the *total* collimation width in the center of rotation:

$$p = \frac{d}{C} = \frac{d}{MS}$$

Recommended by and in:

IEC, International Electrotechnical Commision: Medical electrical equipment – 60601 Part 2-44: Particular requirements for the safety of x-ray equipment for computed tomography. Geneva, Switzerland, 1999.

Examples:

- p=1/3=0.333 means that each z-position is covered by 3 rotations (3-fold overlap)
- p=1 means that the acquisition is not overlapping
- $p=p_{max}$ means that each z-position is covered by half a rotation

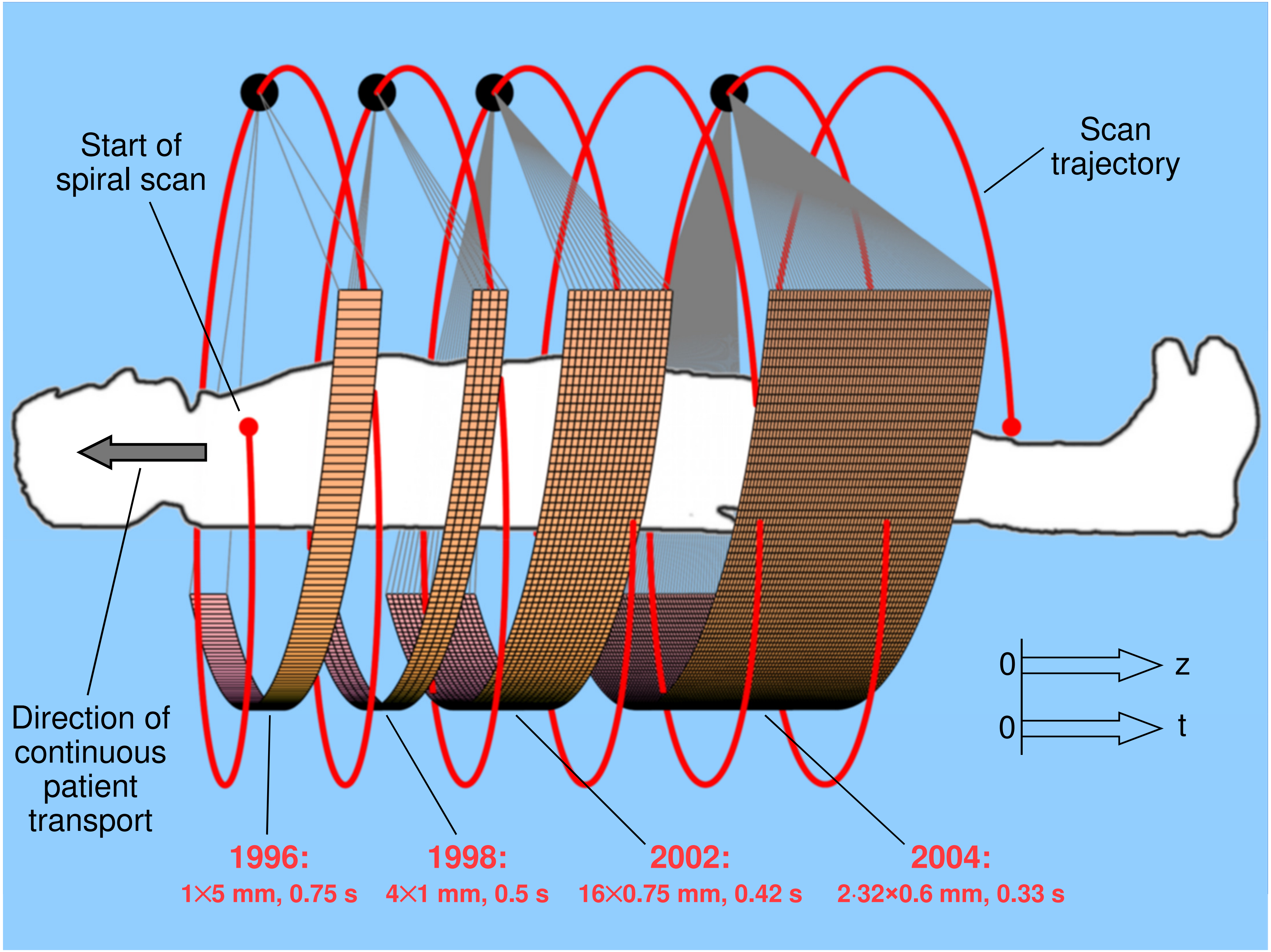
Start of
spiral scan
Scan
trajectory
Direction of
continuous
patient
transport
0
z
0
t
1996:
1×5 mm, 0.75 s
1998:
4×1 mm, 0.5 s
2002:
16×0.75 mm, 0.42 s
2004:
2·32×0.6 mm, 0.33 s

The Cone-Beam Problem

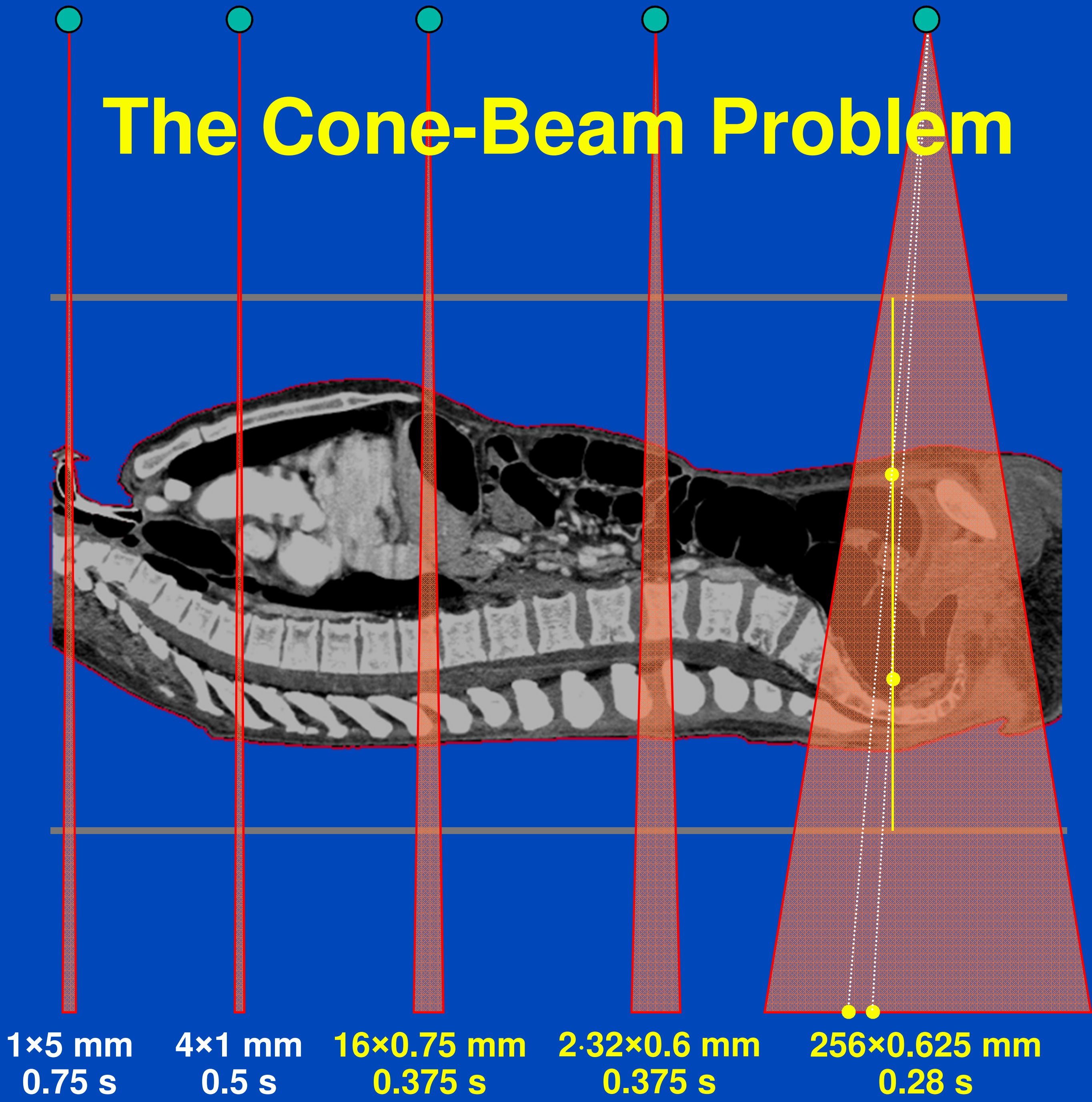

Advanced single-slice rebinning in cone-beam spiral CT

Marc Kachelrieß[a)]
Institute of Medical Physics, University of Erlangen–Nürnberg, Germany

Stefan Schaller
Siemens AG, Medical Engineering Group, Forchheim, Germany

Willi A. Kalender
Institute of Medical Physics, University of Erlangen–Nürnberg, Germany

(Received 11 August 1999; accepted for publication 12 January 2000)

To achieve higher volume coverage at improved *z*-resolution in computed tomography (CT), systems with a large number of detector rows are demanded. However, handling an increased number of detector rows, as compared to today's four-slice scanners, requires to accounting for the cone geometry of the beams. Many so-called cone-beam reconstruction algorithms have been proposed during the last decade. None met all the requirements of the medical spiral cone-beam CT in regard to the need for high image quality, low patient dose and low reconstruction times. We therefore propose an approximate cone-beam algorithm which uses virtual reconstruction planes tilted to optimally fit 180° spiral segments, i.e., the advanced single-slice rebinning (ASSR) algorithm. Our algorithm is a modification of the single-slice rebinning algorithm proposed by Noo *et al.* [Phys. Med. Biol. **44**, 561–570 (1999)] since we use tilted reconstruction slices instead of transaxial slices to approximate the spiral path. Theoretical considerations as well as the reconstruction of simulated phantom data in comparison to the gold standard 180°LI (single-slice spiral CT) were carried out. Image artifacts, *z*-resolution as well as noise levels were evaluated for all simulated scanners. Even for a high number of detector rows the artifact level in the reconstructed images remains comparable to that of 180°LI. Multiplanar reformations of the Defrise phantom show none of the typical cone-beam artifacts usually appearing when going to larger cone angles. Image noise as well as the shape of the respective slice sensitivity profiles are equivalent to the single-slice spiral reconstruction, *z*-resolution is slightly decreased. The ASSR has the potential to become a practical tool for medical spiral cone-beam CT. Its computational complexity lies in the order of standard single-slice CT and it allows to use available 2D backprojection hardware. [S0094-2405(00)00804-X]

Key words: computed tomography (CT), spiral CT, multi-slice CT, cone-beam detector systems, 3D reconstruction

ASSR: Advanced Single-Slice Rebinning

3D and 4D Image Reconstruction for Medium Cone Angles

- First practical solution to the cone-beam problem in medical CT
- Reduction of 3D data to 2D slices
- Commercially implemented as AMPR
- ASSR is recommended for up to 64 slices

Do not confuse
the transmission algorithm ASSR
with
the emission algorithm SSRB!

The ASSR Algorithm

$$p = \frac{d}{MS} \leq 1.5$$

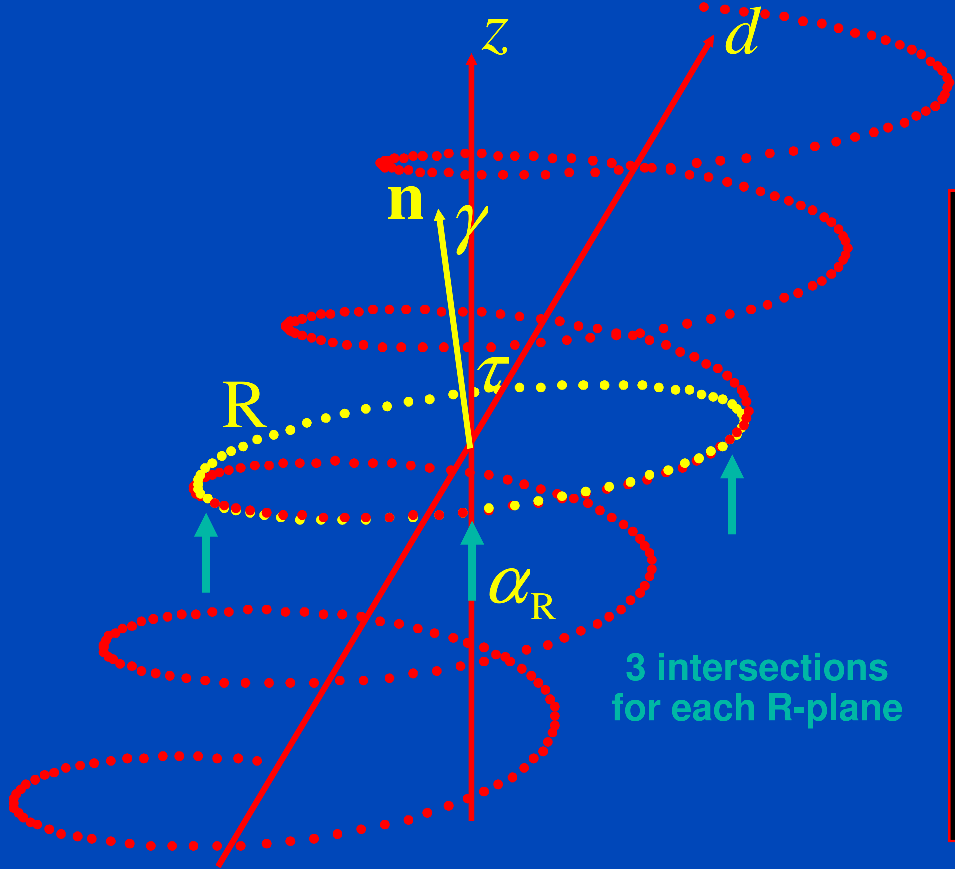

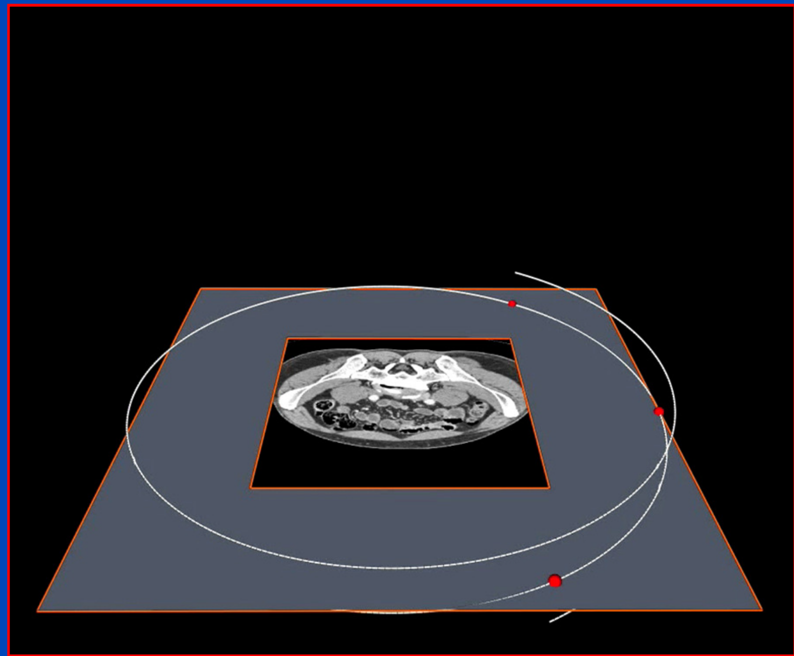

Mean deviation at distance R_M: $\Delta \approx 0.007 \cdot d$

at distance R_F: $\Delta \approx 0.014 \cdot d$

Comparison to Other Approximate Algorithms

180°LI d=1.5mm | Π d=64mm | MFR d=64mm | ASSR d=64mm

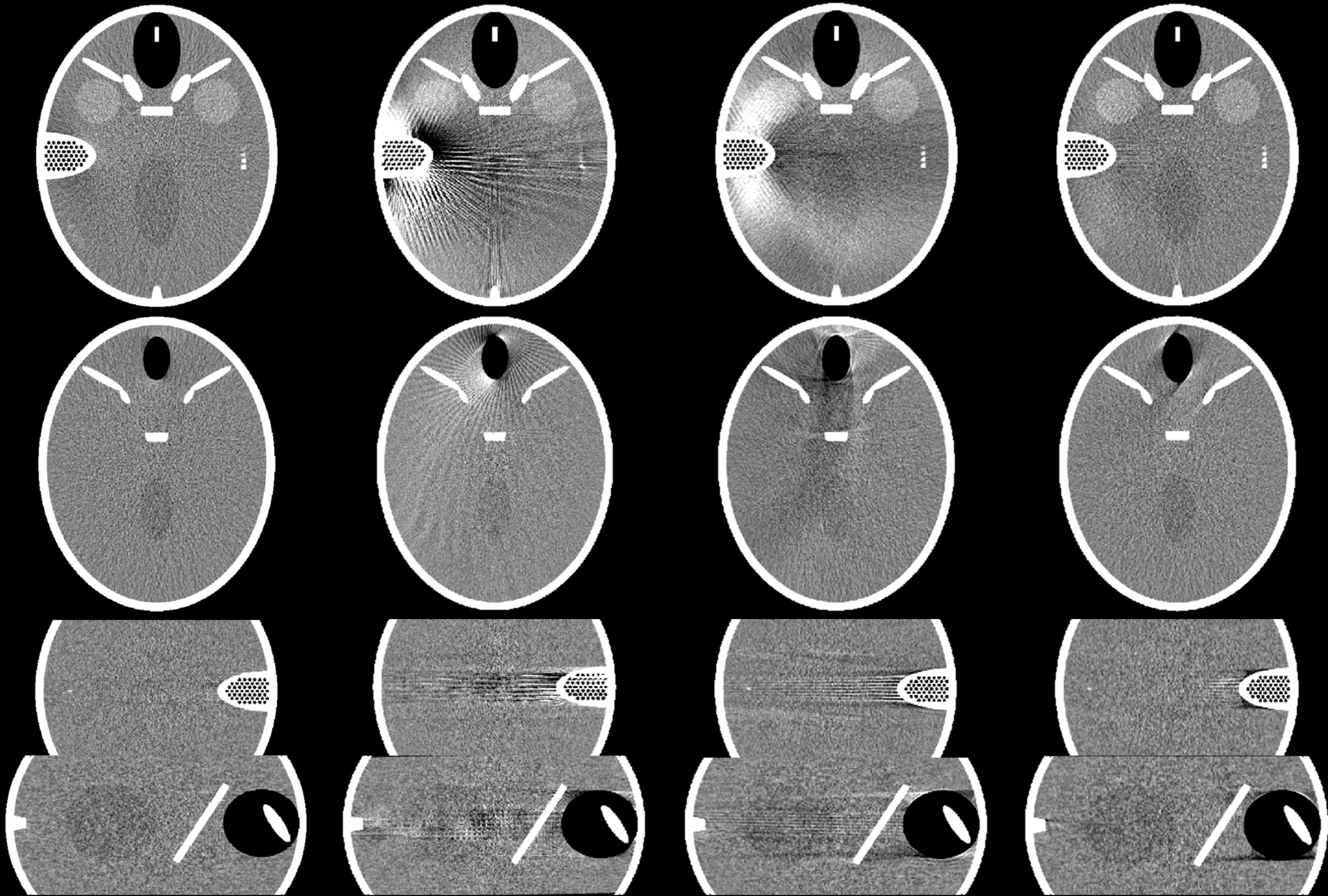

Patient Images with ASSR

- High image quality
- High performance
- Use of available 2D reconstruction hardware
- 100% detector usage
- Arbitrary pitch

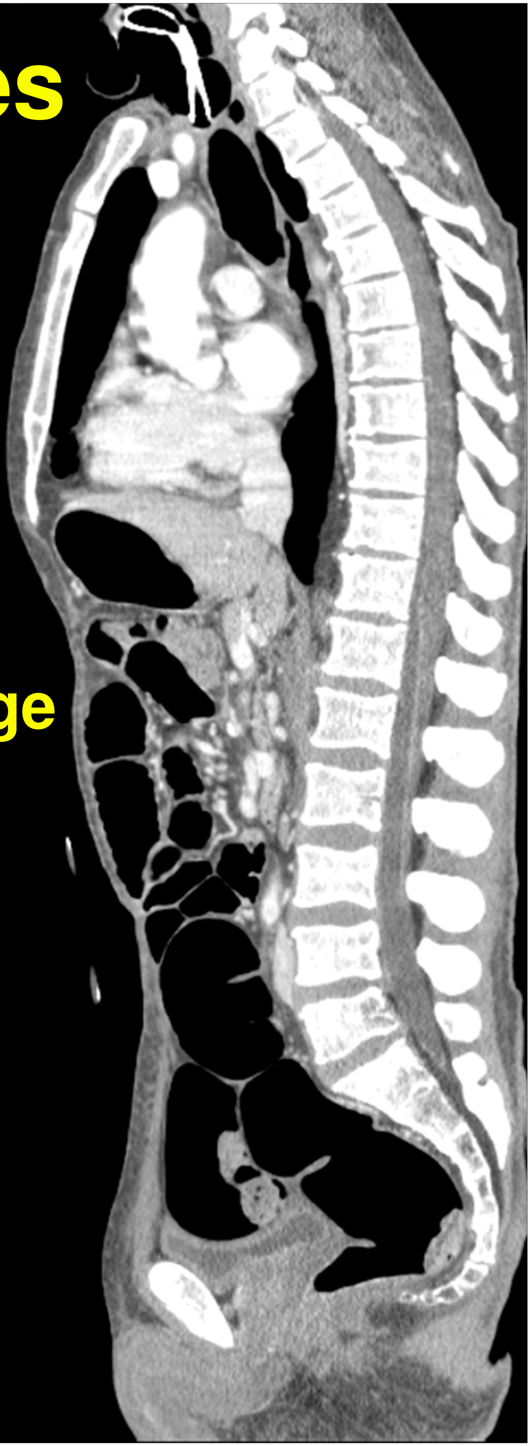

- Sensation 16
- 0.5 s rotation
- 16×0.75 mm collimation
- pitch 1.0
- 70 cm in 29 s
- 1.4 GB rawdata
- 1400 images

CT-Angiography
Sensation 64 spiral scan with 2·32×0.6 mm and 0.375 s

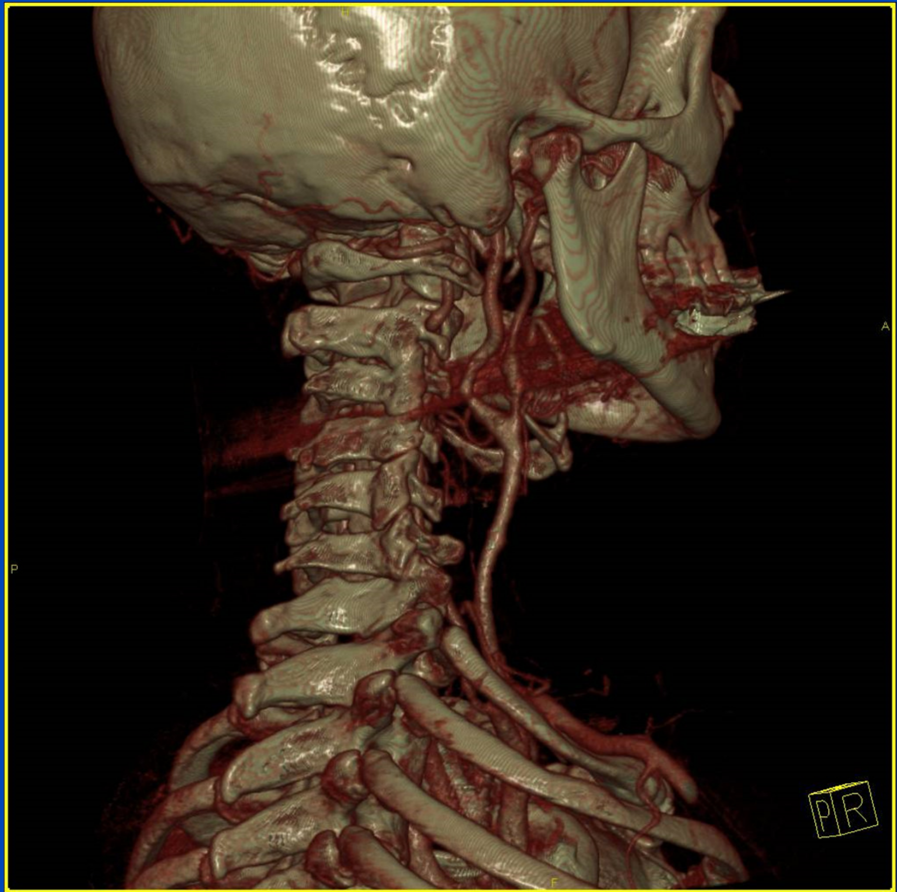

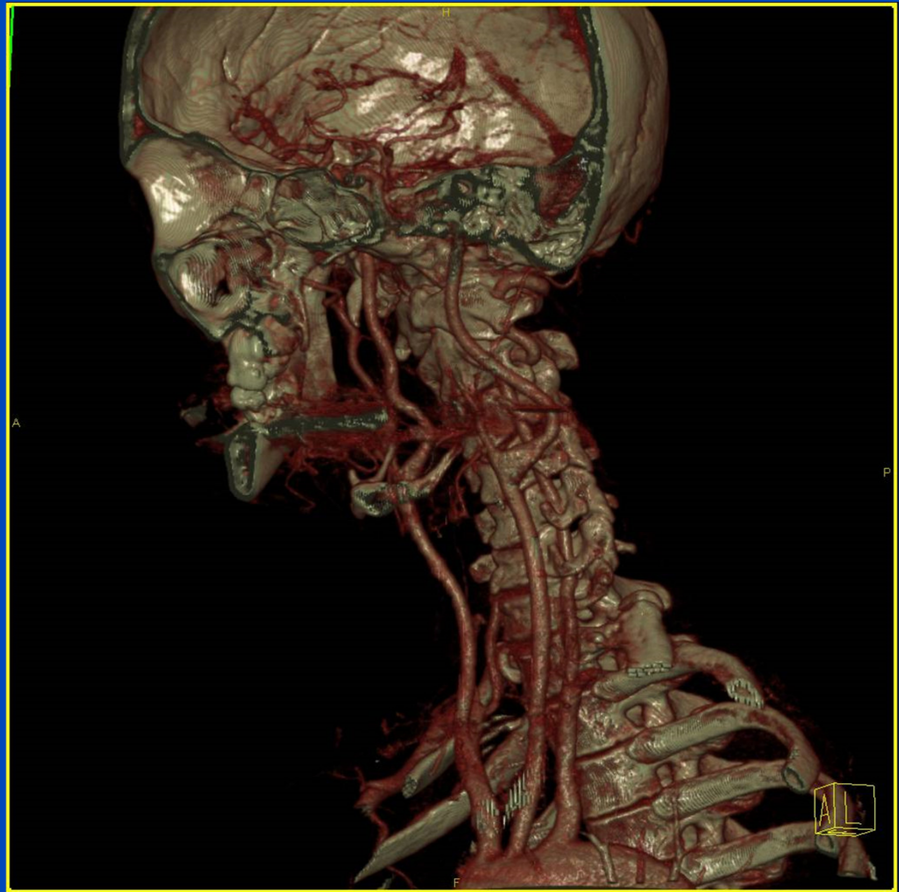

Feldkamp-Type Reconstruction

- Approximate
- Similar to 2D reconstruction:
  - row-wise filtering of the rawdata
  - followed by backprojection
- True 3D volumetric backprojection along the original ray direction
- Compared to ASSR:
  - larger cone-angles possible
  - lower reconstruction speed
  - requires 3D backprojection hardware

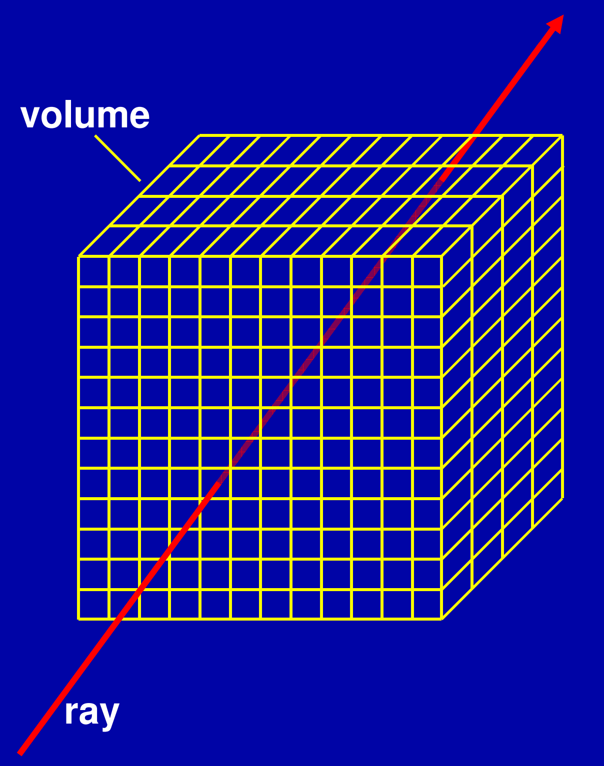

3D backprojection

dkfz.

Perspective Geometry

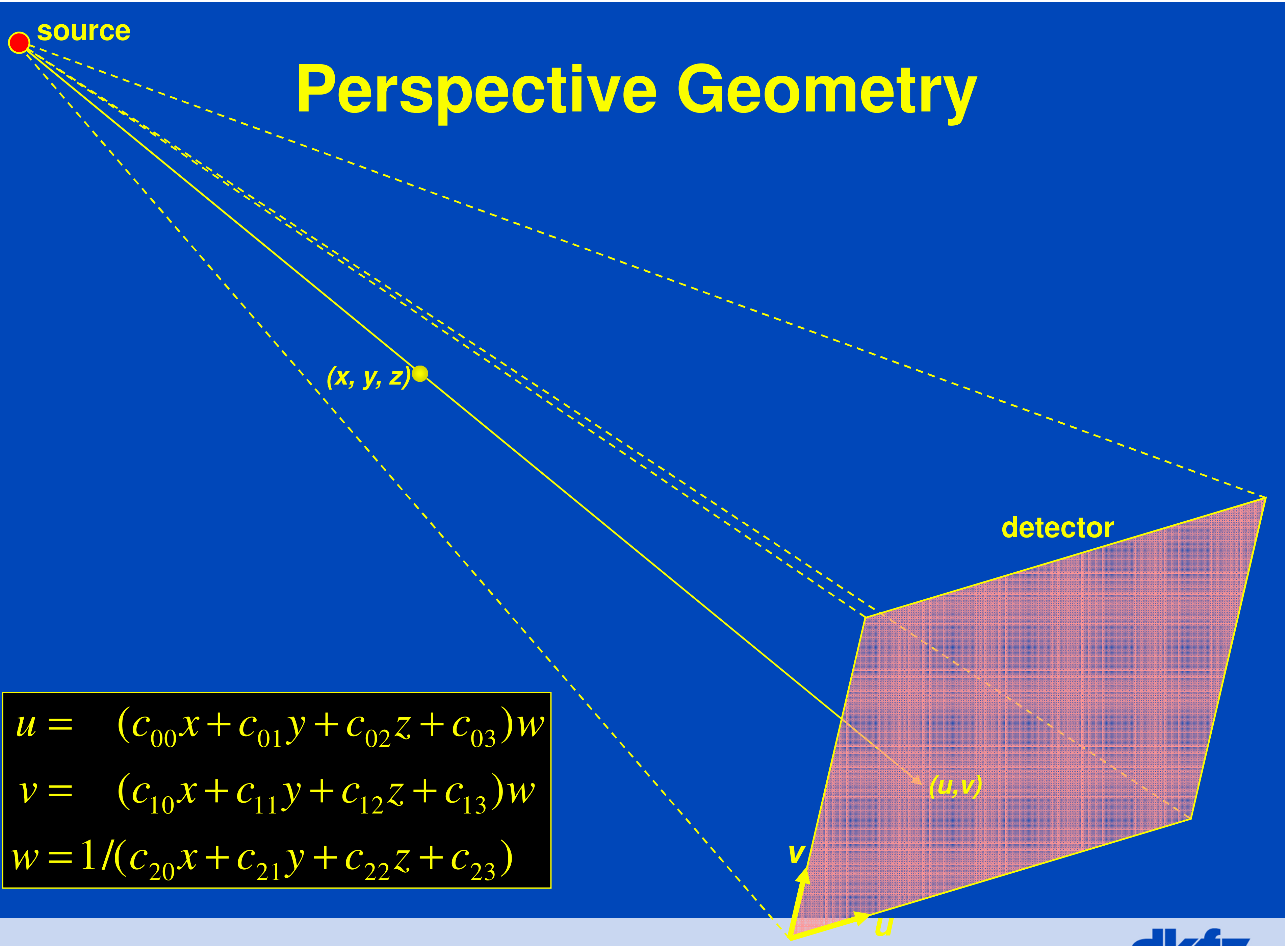

$$u = \quad (c_{00}x + c_{01}y + c_{02}z + c_{03})w$$

$$v = \quad (c_{10}x + c_{11}y + c_{12}z + c_{13})w$$

$$w = 1/(c_{20}x + c_{21}y + c_{22}z + c_{23})$$

Cone-Beam Artifacts

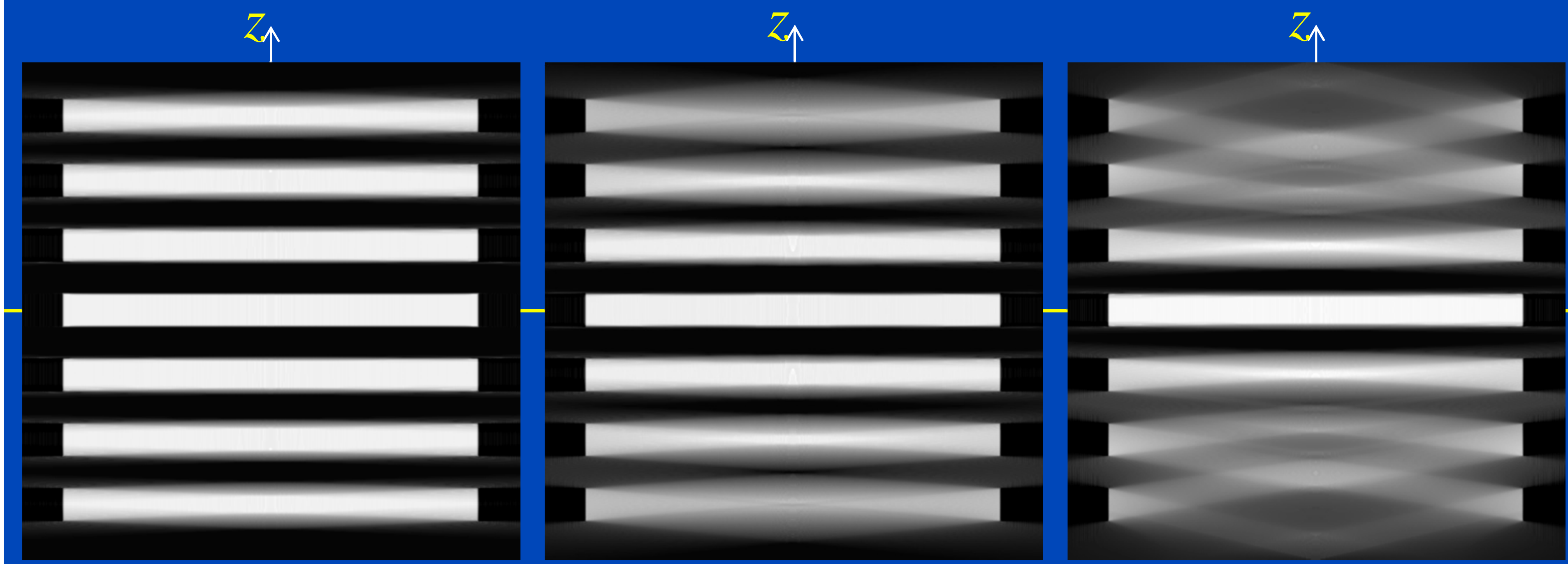

Cone-angle Γ = 6° Cone-angle Γ = 14° Cone-angle Γ = 28°

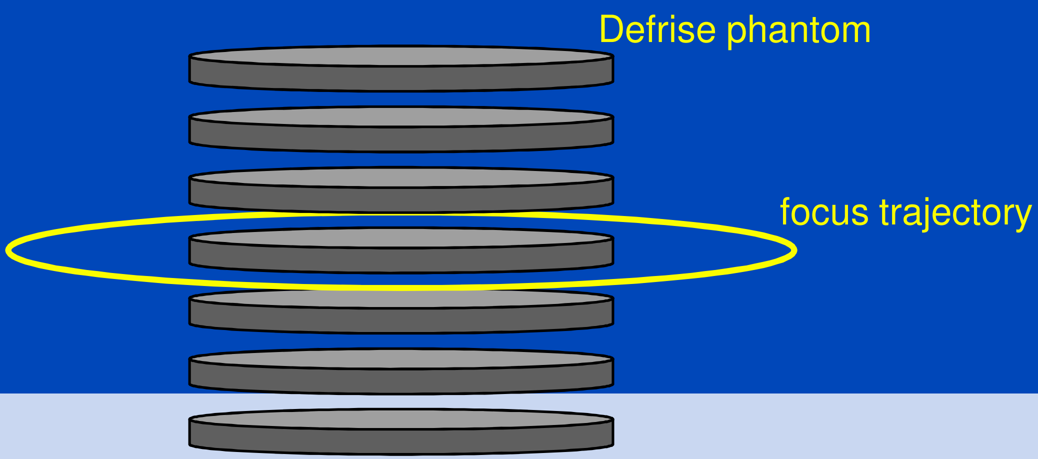

Extended parallel backprojection for standard three-dimensional and phase-correlated four-dimensional axial and spiral cone-beam CT with arbitrary pitch, arbitrary cone-angle, and 100% dose usage

Marc Kachelrieß,[a] Michael Knaup, and Willi A. Kalender
Institute of Medical Physics, University of Erlangen—Nürnberg, Germany

(Received 12 September 2003; revised 7 April 2004; accepted for publication 7 April 2004; published 27 May 2004)

We have developed a new approximate Feldkamp-type algorithm that we call the extended parallel backprojection (EPBP). Its main features are a phase-weighted backprojection and a voxel-by-voxel 180° normalization. The first feature ensures three-dimensional (3-D) and 4-D capabilities with one and the same algorithm; the second ensures 100% detector usage (each ray is accounted for). The algorithm was evaluated using simulated data of a thorax phantom and a cardiac motion phantom for scanners with up to 256 slices. Axial (circle and sequence) and spiral scan trajectories were investigated. The standard reconstructions (EPBPStd) are of high quality, even for as many as 256 slices. The cardiac reconstructions (EPBPCI) are of high quality as well and show no significant deterioration of objects even far off the center of rotation. Since EPBPCI uses the cardio interpolation (CI) phase weighting the temporal resolution is equivalent to that of the well-established single-slice and multislice cardiac approaches 180°CI, 180°MCI, and ASSRCI, respectively, and lies in the order of 50 to 100 ms for rotation times between 0.4 and 0.5 s. EPBP appears to fulfill all required demands. Especially the phase-correlated EPBP reconstruction of cardiac multiple circle scan data is of high interest, e.g., for dynamic perfusion studies of the heart. [DOI: 10.1118/1.1755569]

Key words: Cone-beam CT (CBCT), cardiac imaging, 4-D reconstruction, image quality

I. INTRODUCTION

The ongoing development of medical cone-beam CT (CBCT) scanners requires providing cone-beam reconstruction algorithms adequate for medical purposes. These must adopted and used to reconstruct cardiac data for scanners with more than four slices.

However, there are several restrictions to these approaches that may inhibit their use in scanners with signifi-

Extended Parallel Backprojection (EPBP)

3D and 4D Feldkamp-Type Image Reconstruction for Large Cone Angles

- Trajectories: circle, sequence, spiral
- Scan modes: standard, phase-correlated
- Rebinning: azimuthal + longitudinal + radial
- Feldkamp-type: convolution + true 3D backprojection
- 100% detector usage
- Fast and efficient

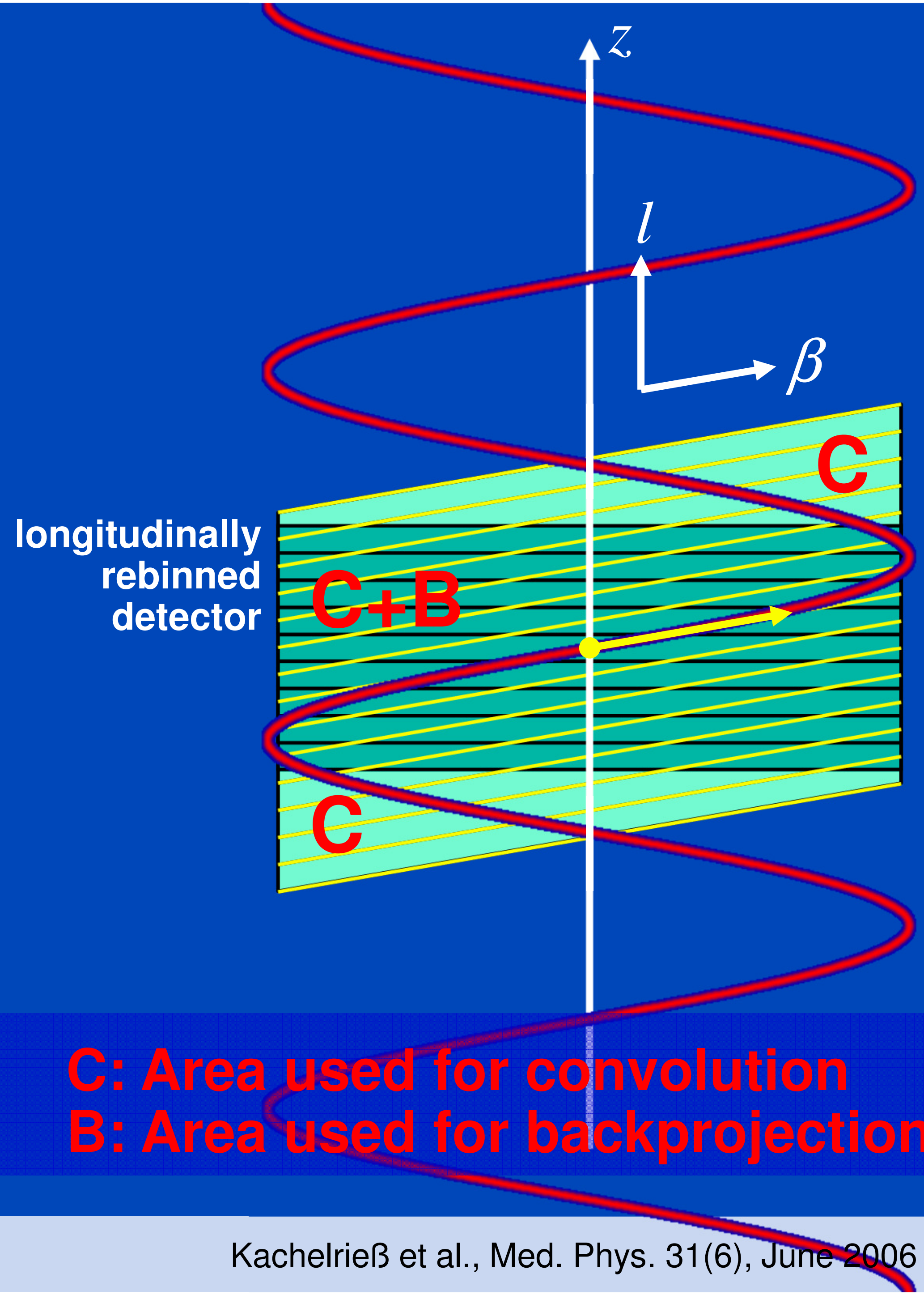

$$p = \frac{d}{MS} \leq 1.5$$

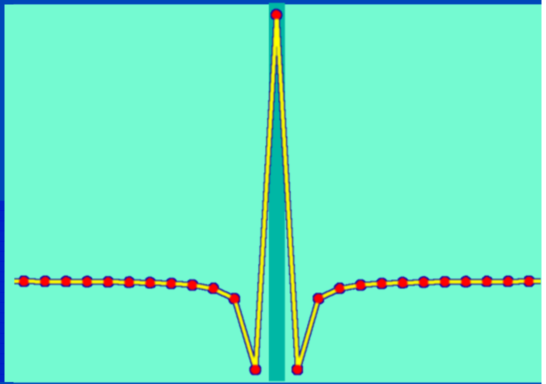

C: Area used for convolution
B: Area used for backprojection

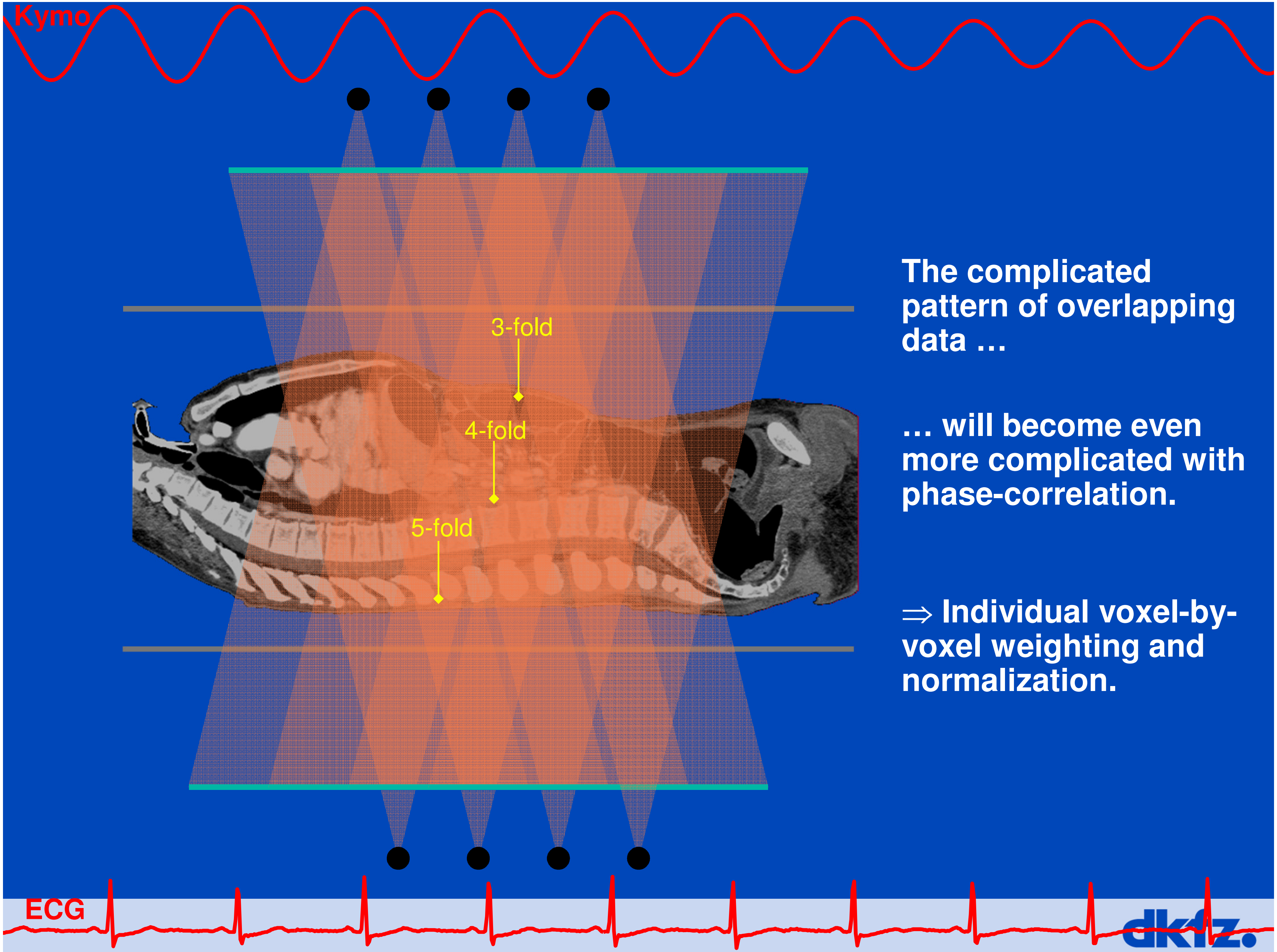

The complicated pattern of overlapping data …

… will become even more complicated with phase-correlation.

⇒ Individual voxel-by-voxel weighting and normalization.

The 180° Condition

$$\int d\vartheta\, w(\vartheta) = \pi$$

and

$$\sum_k w(\vartheta + k\pi) = 1$$

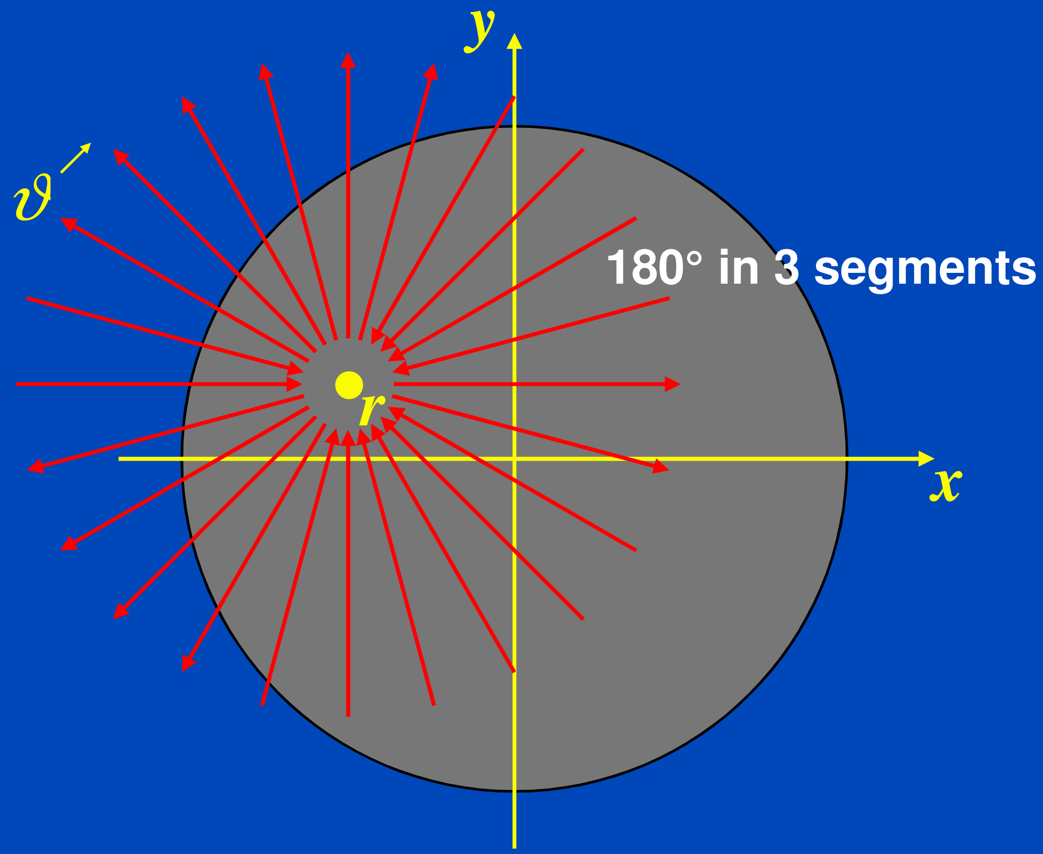

The (weighted) contributions to each object point must make up an interval of 180° and weight 1.

- Spiral
- EPBP Std
- *p* = 0.375

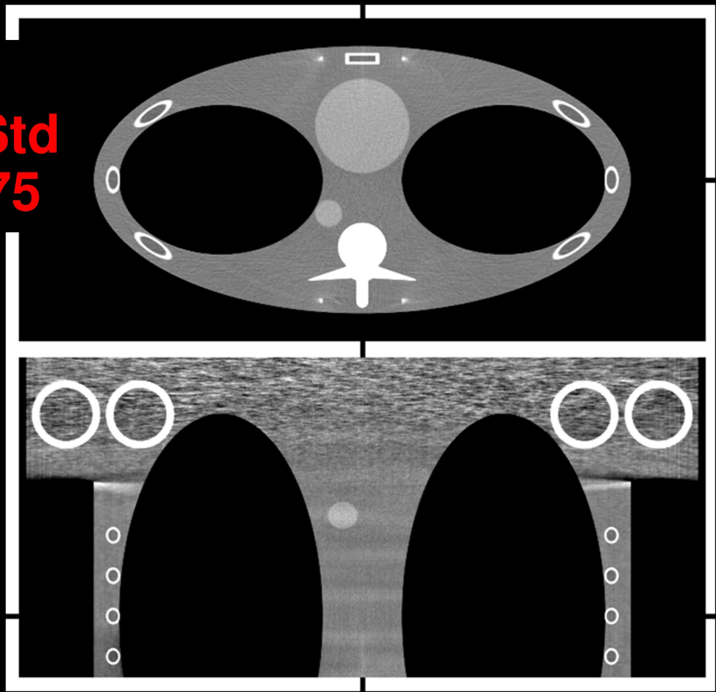

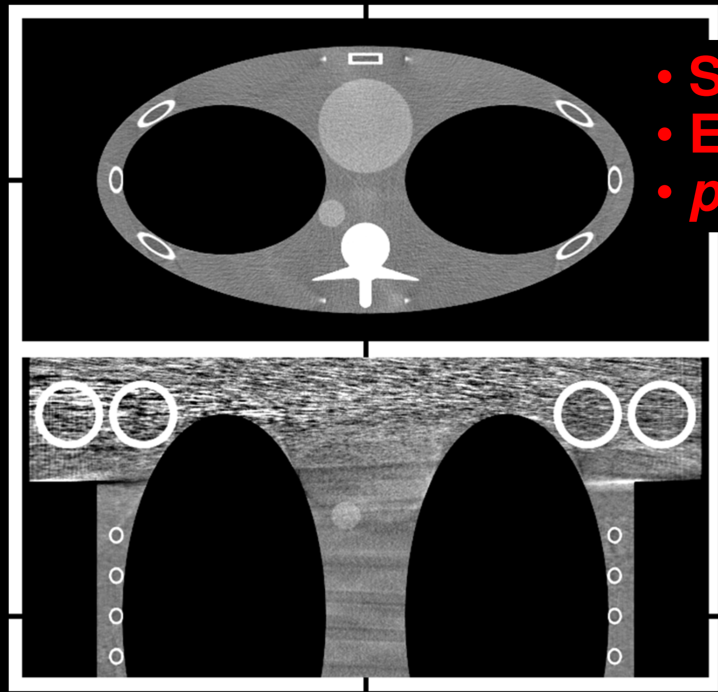

- Spiral
- EPBP Std
- *p* = 1.0

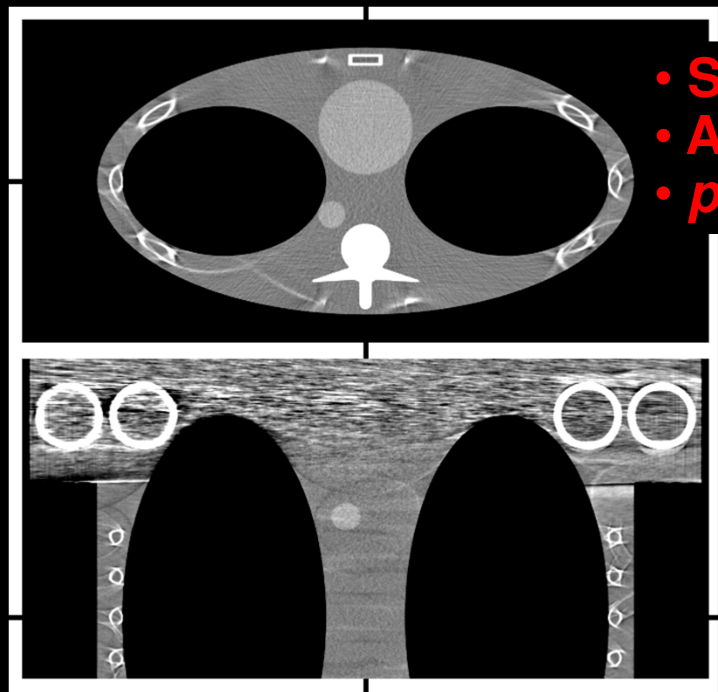

- Spiral
- ASSR Std
- *p* = 1.0

- 256 slices
- (0/300)

Kachelrieß et al., Med. Phys. 31(6): 1623-1641, 2004

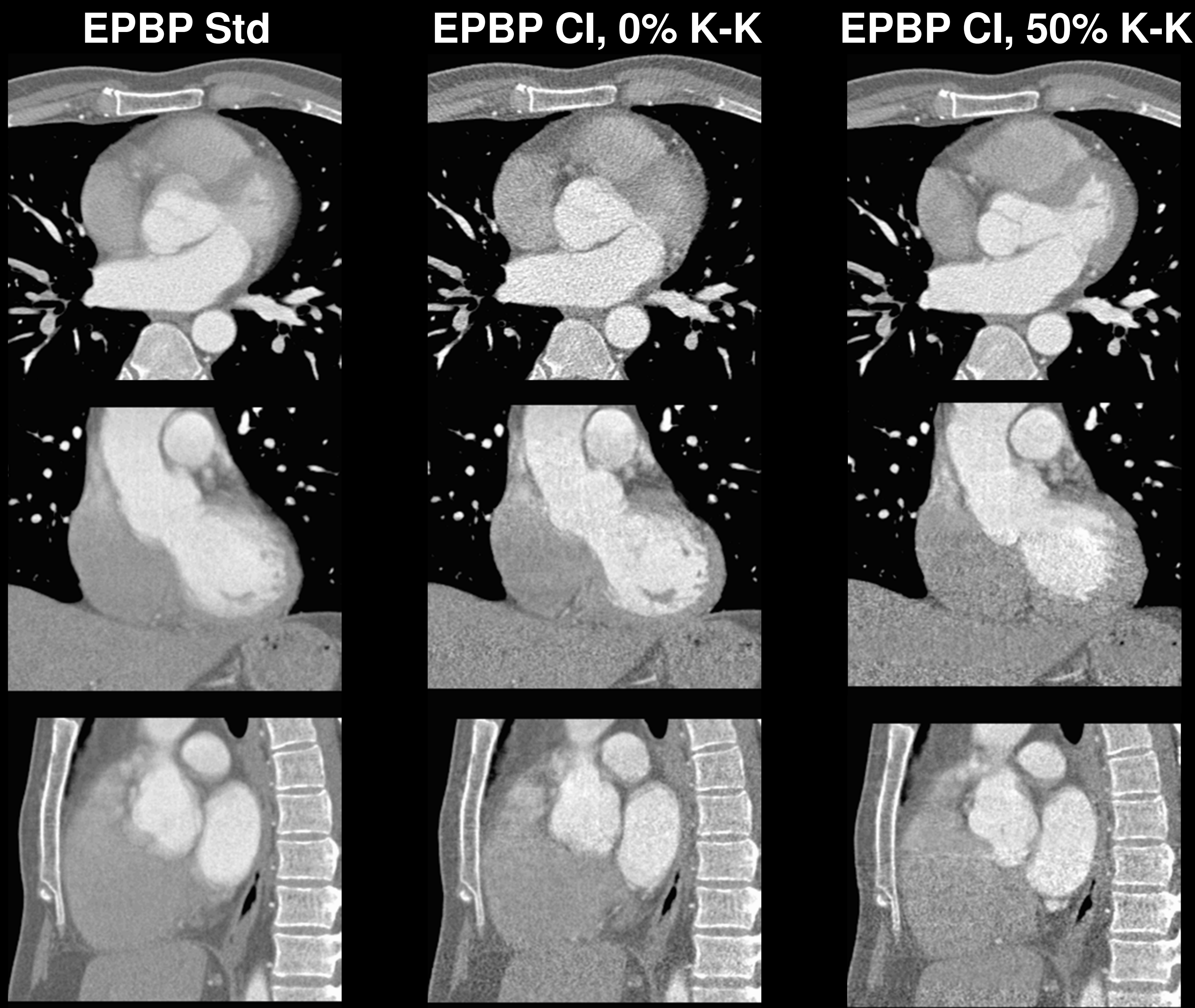

Patient example, 32x0.6 mm, z-FFS, p=0.23, t_{rot}=0.375 s.

normalized

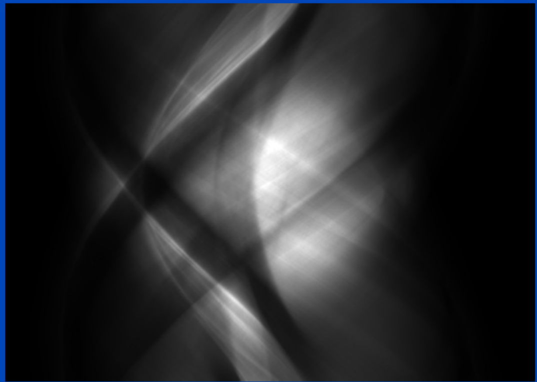

log normalized

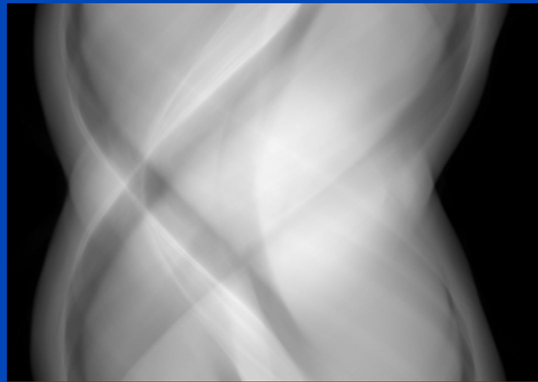

log normalized and convolved

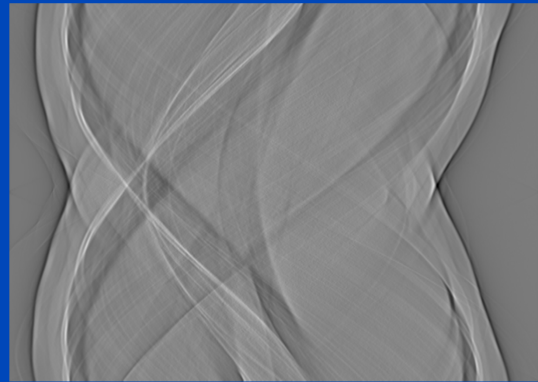

after 36°

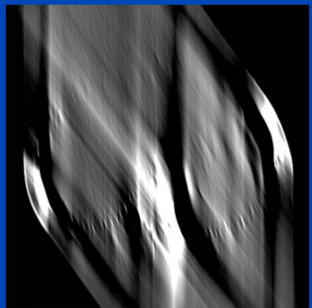

after 72°

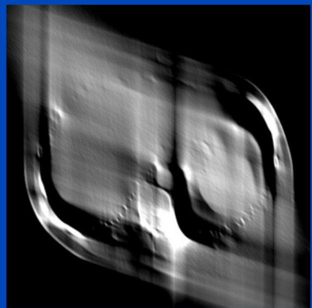

after 108°

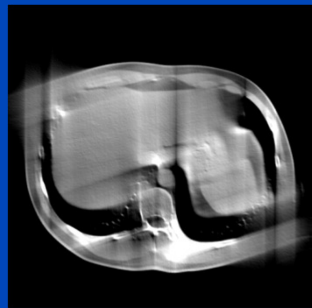

after 144°

after 180°

1 projection

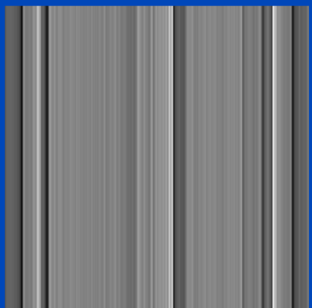

2 projections

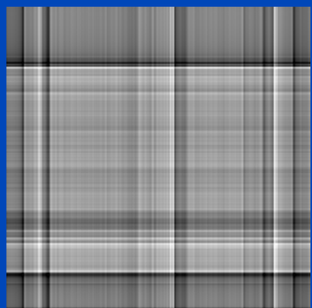

4 projections

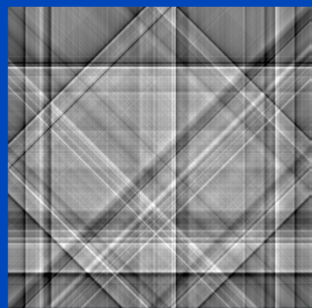

8 projections

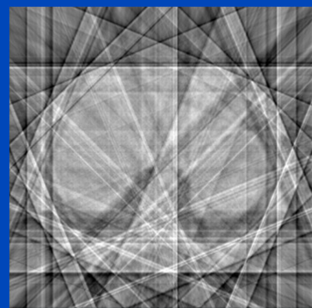

all projections

Analytical Reconstruction: Gridding and Fourier Reconstruction

$$F(u_m \cos \vartheta_n, u_m \sin \vartheta_n)$$

$$F(\boldsymbol{u}_i)$$

$$f(\boldsymbol{r}) = ?$$

Resampling

This type of resampling is called *destination-driven* resampling.

**Destination domain:
This is were you
would like to know
the data!**

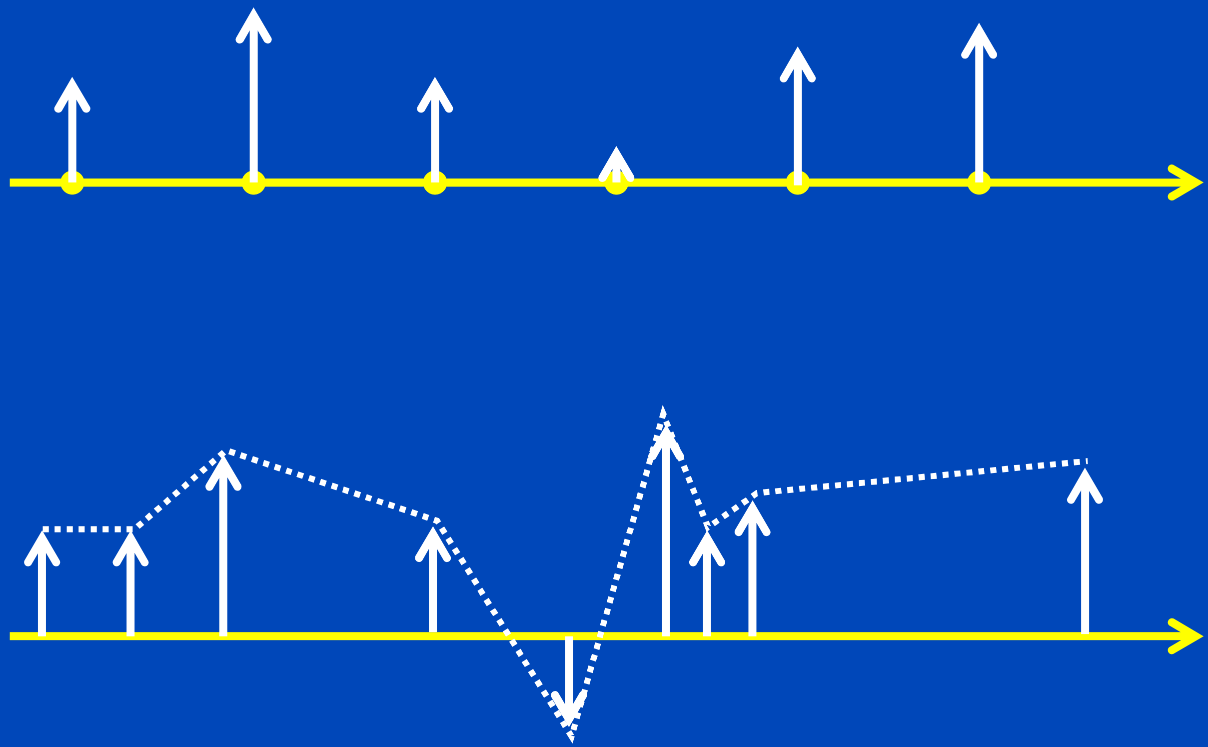

**Source domain:
The samples that you
have measured!**

Resampling

This type of resampling is called *source-driven* resampling.

Destination domain: This is were you would like to know the data!

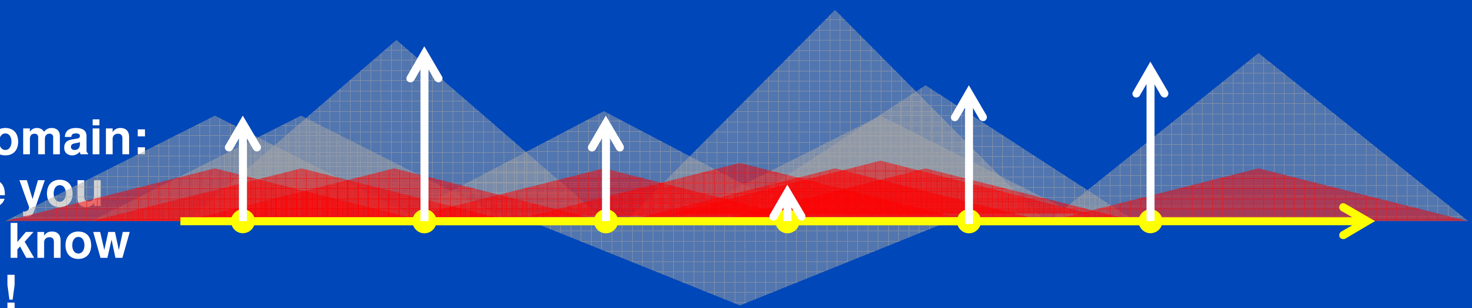

Source domain: The samples that you have measured!

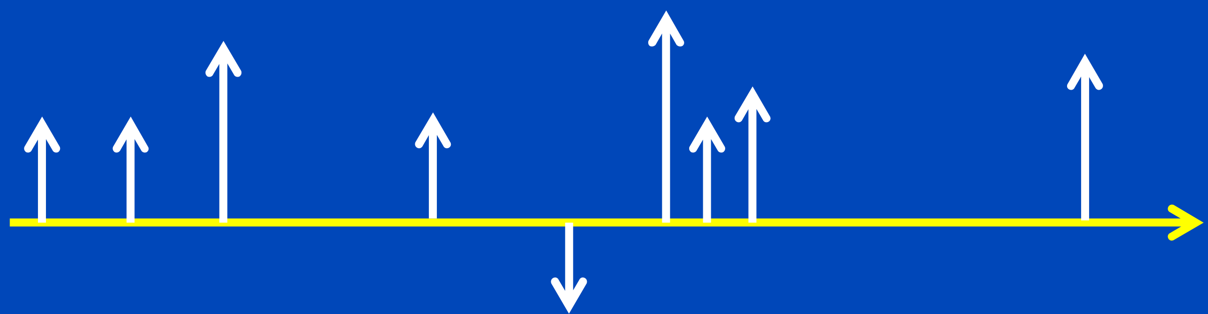

DD Resampling in 1D

- Function $G(v)$ known at $v = v_0 + n\,\Delta v$ for $n = 1, \ldots, N$.
- We would like to know $F(u) = G(v(u))$ at discrete points $u = u_0 + m\,\Delta u$ for $m = 1, \ldots, M$, with $v(u)$ being a non-linear coordinate transform.
- How should we obtain $F(u)$?
- Interpolation:

$$F(u) = (G * K)(v(u))$$

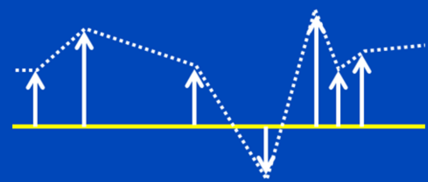

- Typical interpolation kernels

$$K_{\mathrm{NN}}(v) = \frac{1}{\Delta v}\,\mathrm{II}(\frac{v}{\Delta v})$$

$$K_{\mathrm{LI}}(v) = \frac{1}{\Delta v}\,\Lambda(\frac{v}{\Delta v})$$

DD Resampling in 1D

- What is the influence of the interpolation kernel?
- In the original domain, the kernel introduces a small scale local error (e.g. a slight smoothing), which may have the advantage of reducing aliasing.
- However, after a Fourier transform, small scale errors convert into large scale errors.
- Regard the kernel influence in spatial domain:

$$f(x) = \int du\, F(u) e^{2\pi i u x} = \int du\, (G * K)(v(u)) e^{2\pi i u x}$$

- Due to the non-linear coordinate transform the kernel influence cannot be appreciated in the spatial domain. Large scale errors will remain.
- Interpolation is not the method of choice if the data are needed in the other domain!

dkfz.

SD Resampling (Gridding) in 1D

- **Let us make the operation linear in *u* rather than in *v*:**

$$F(u) * W(u) = \int d\hat{u}\, F(\hat{u}) W(u - \hat{u})$$

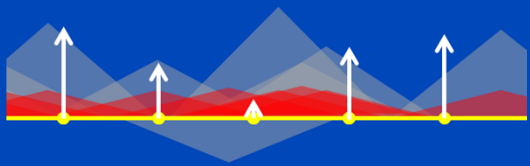

$$= \int dv \left|\frac{\partial u}{\partial v}\right| F(u(v)) W(u - u(v))$$

$$= \int dv \left|\frac{\partial u}{\partial v}\right| G(v) W(u - u(v))$$

- **In spatial domain we now have**

$$f(x) w(x) = \int du\, (F * W)(u) e^{2\pi i u x}$$

- **Dividing by w(x) removes the influence of the window.**
- **This way of resampling is known as gridding.**

Gridding (SD Resampling) in 1D

- How to choose the gridding window?
- Sampling at $u = u_0 + m\,\Delta u$ in frequency domain

$$(F * W)(u)\frac{1}{\Delta u}\,\mathrm{III}(\frac{u - u_0}{\Delta u})$$

introduces periodic repetitions in spatial domain:

$$(fw)(x) * \mathrm{III}(\Delta u x)e^{2\pi i u_0 x}$$

- To avoid aliasing the window must be constrained to a support of $1/\Delta u$.

Window functions

- **Good window functions are**

$$w_c^{\mathrm{KB}}(x) = \operatorname{sinc}(\sqrt{x^2 - c^2})$$

$$W_c^{\mathrm{KB}}(u) = \mathrm{II}(u) I_0(\pi c \sqrt{1 - 4u^2})$$

$$\operatorname{sinc} x = \frac{\sin \pi x}{\pi x}$$

$$\operatorname{sinc} ix = \frac{\sinh \pi x}{\pi x}$$

$$w_c^{\mathrm{VdM}}(x) = \cos(\pi \sqrt{x^2 - c^2})$$

$$W_c^{\mathrm{VdM}}(u) = \mathrm{II}(u) \frac{I_1(\pi c \sqrt{1 - 4u^2})}{\sqrt{1 - 4u^2}} \pi c + \tfrac{1}{2} \sum_{\pm} \delta(u \pm \tfrac{1}{2}).$$

- **To design a window that covers *k* = 4 sampling points in Fourier domain, use**

$$W(u) = W_c\left(\frac{u}{k \Delta u}\right)$$

Bessel and Modified Bessel Function

$$J_n(x) = \frac{(-i)^n}{\pi} \int_0^\pi d\vartheta \, \cos n\vartheta \, e^{ix \cos\vartheta} = \sum_{k=0}^\infty \frac{(-)^k (x/2)^{n+2k}}{k! \, \Gamma(n+k+1)}$$

$$I_n(x) = i^{-n} J_n(ix)$$

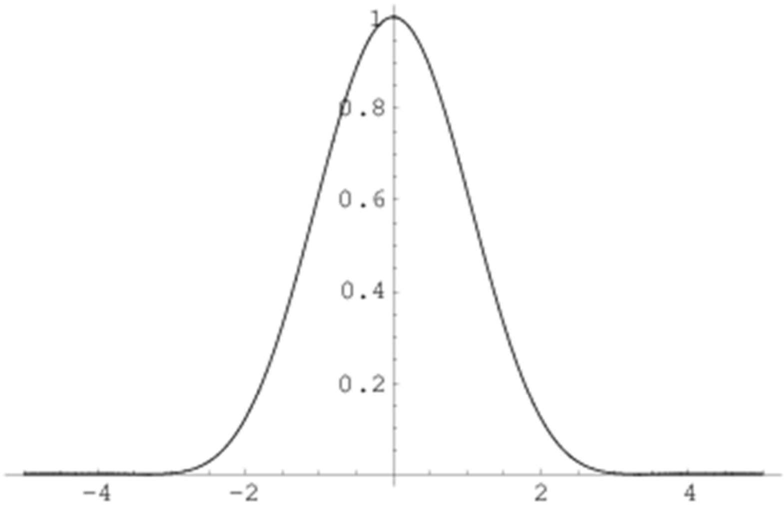

(a) $w_3^{\mathrm{KB}}(x)/w_3^{\mathrm{KB}}(0)$

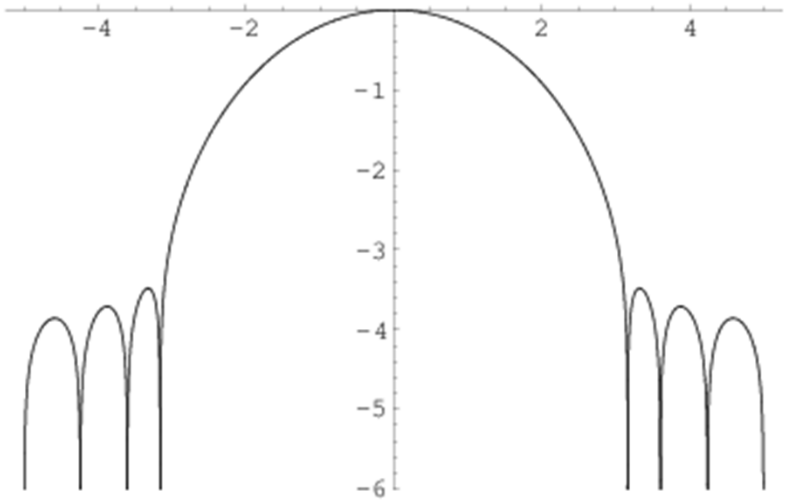

(b) $\lg|w_3^{\mathrm{KB}}(x)/w_3^{\mathrm{KB}}(0)|$

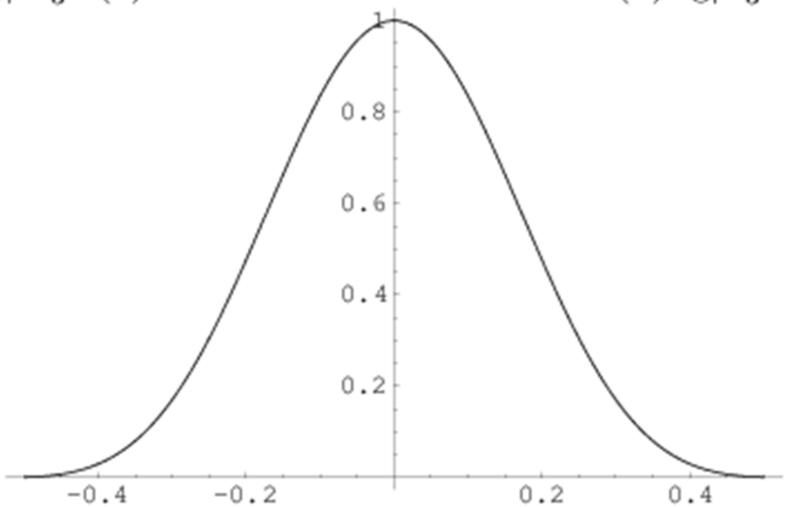

(c) $W_3^{\mathrm{KB}}(u)/W_3^{\mathrm{KB}}(0)$

Gridding in 2D
Here: From Radial Samples

- **Fourier slice theorem**

$$P(\vartheta, \rho) = F(\rho \cos\vartheta, \rho \sin\vartheta)$$

- **Gridding**

$$(F * W)(u, v) = \int d\hat{u} d\hat{v}\, F(\hat{u}, \hat{v}) W(u - \hat{u}, v - \hat{v})$$

$$= \int d\rho d\vartheta\, |\rho| F(\rho \cos\vartheta, \rho \sin\vartheta) W(u - \rho\cos\vartheta, v - \rho\sin\vartheta)$$

$$= \int d\rho d\vartheta\, |\rho| P(\vartheta, \rho) W(u - \rho\cos\vartheta, v - \rho\sin\vartheta)$$

- **Inverse Fourier transform**

$$f(x, y) w(x, y) = \int du dv\, (F * W)(u, v) e^{2\pi i (ux + vy)}$$

Gridding in 2D

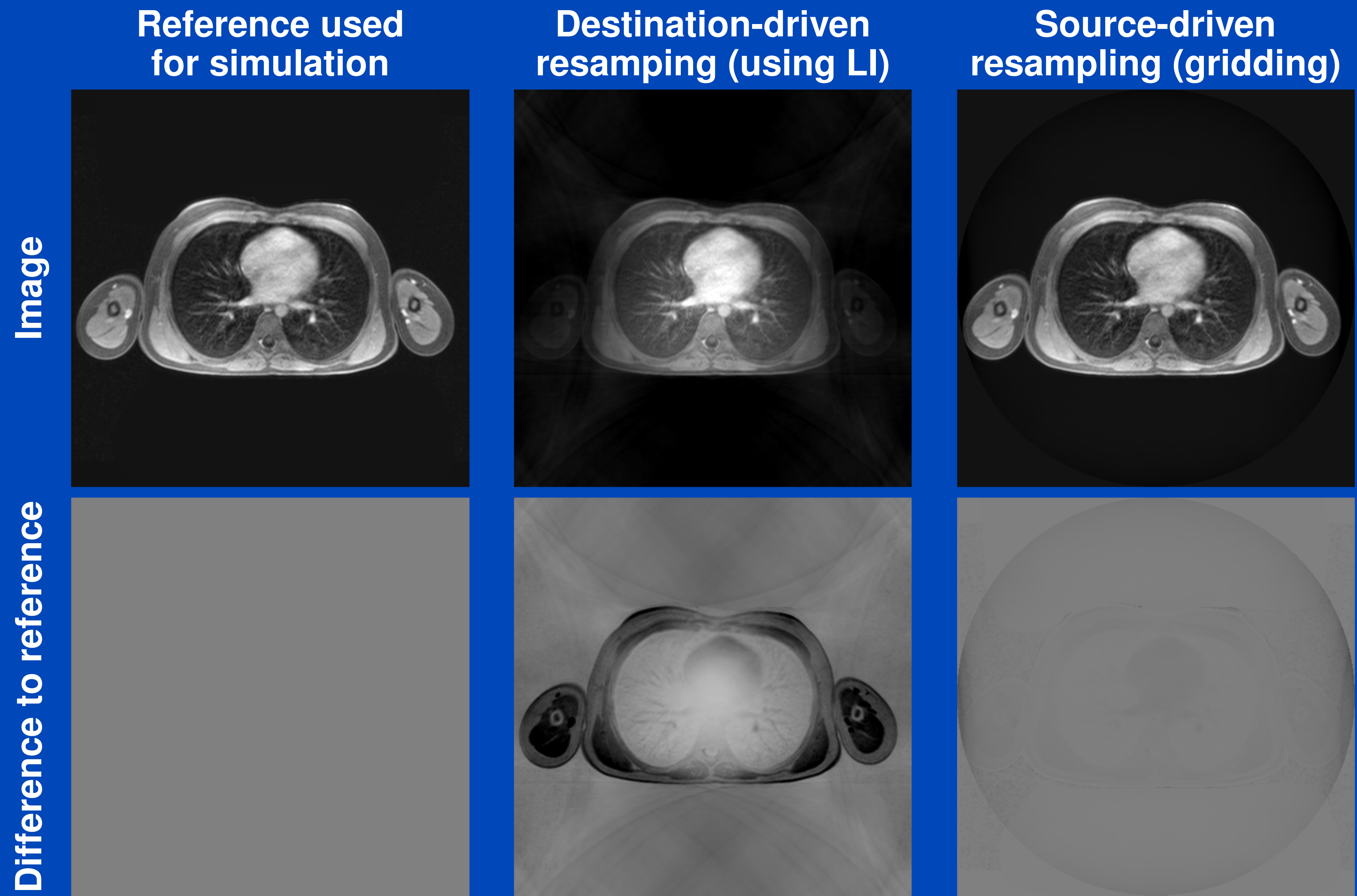

MR simulation with 640 radial spokes

Analytical CT Reconstruction

- Filtered backprojection
- Variants of FBP for use with spiral trajectories
- Variants of FBP for use with cardiac gating
- No Fourier reconstruction
  - on discrete data only FBP is numerically exact
  - FBP is faster for image sizes up to about 1024^2 or 2048^2
  - Fourier recon does not work for cone-beam CT

Analytical MR Reconstruction

- Fourier inversion (from cartesian k-space trajectories)
- Fourier reconstruction (with gridding)
- Gridding-based reconstruction from arbitrary k-space trajectories

Analytical 2D PET Reconstruction

- **Projections (modeled as line integrals)**

$$p(\vartheta, \xi) = \int dx dy \, \lambda(x, y) \delta(x \cos \vartheta + y \sin \vartheta - \xi)$$

- **Filtered backprojection (FBP)**

Convolution kernel (filter)

$$\lambda(x, y) = \int_0^{\pi} d\vartheta \, p(\xi, \vartheta) * k(\xi) \big|_{\xi = x \cos \vartheta + y \sin \vartheta}$$

Activity distribution

- **Quantitative corrections of the projection data necessary before reconstruction!**

Quantification: SUV

- Standardized uptake value:

$$SUV(\boldsymbol{x},t) = \frac{c(\boldsymbol{x},t)}{A(t)/W}$$

  - *c*: local activity concentration [kBq/mL]
  - *A*: total activity [kBq]
  - *W*: patient weight [g]

$\Rightarrow$ Units of SUV are g/mL (or dimensionless under the assumption that 1 g of tissue corresponds to 1 mL)

- Uniform activity distribution: SUV = 1.0
- Some tumors: SUV up to 25.0

Attenuation

- The annihilation photons are attenuated when traversing the patient (and the system hardware).

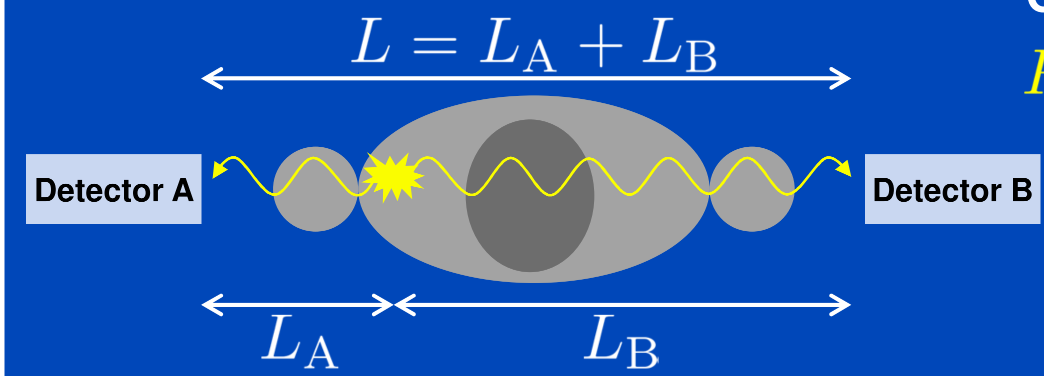

Coincidence probability:

$$P = P(L_\mathrm{A}) \cdot P(L_\mathrm{B})$$

$$= e^{-\int_{L_\mathrm{A}} d^3r\,\mu(\boldsymbol{r})} \cdot e^{-\int_{L_\mathrm{B}} d^3r\,\mu(\boldsymbol{r})}$$

$$= e^{-\int_{L} d^3r\,\mu(\boldsymbol{r})}$$

Independent of annihilation event location!

- The number of detectable coincidence events for each LOR *j* is reduced by the attenuation factor

$$AF_j = e^{-\int_{L} d^3r\,\mu(\boldsymbol{r})} \qquad AF(30\,\mathrm{cm}\ \mathrm{H_2O}) \approx 0.05$$

Attenuation correction (AC) necessary!

NAC vs. AC

Ga68 - Measured Data (1)

Non Attenuation-corrected Image (NAC)

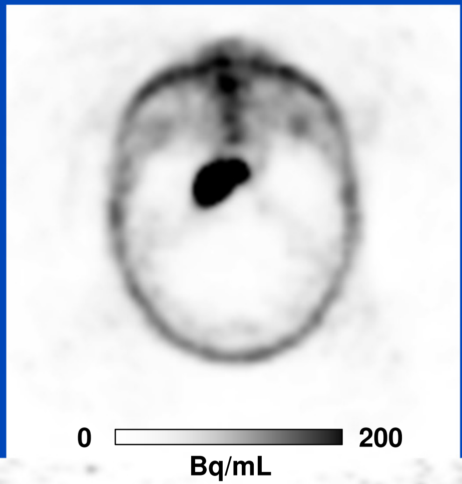

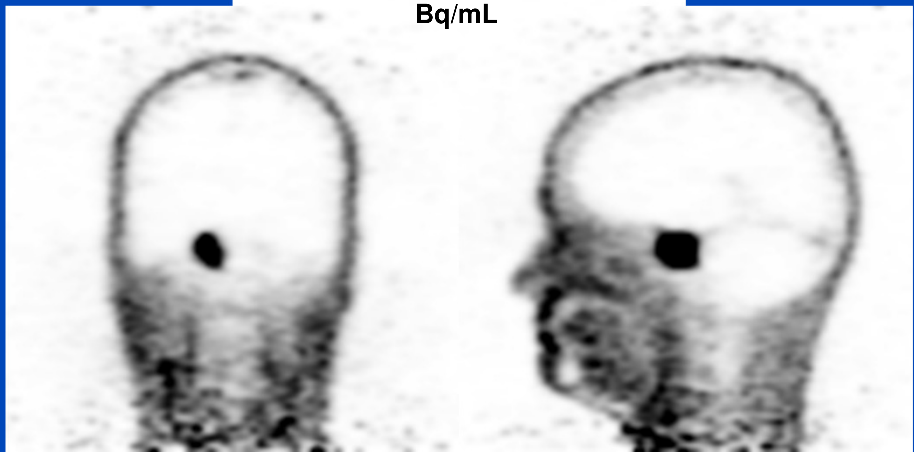

Half-life:
$T_{1/2} = 68$ min

Attenuation-corrected Images (AC)

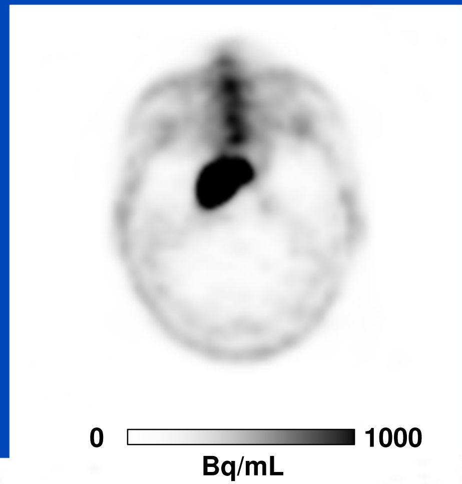

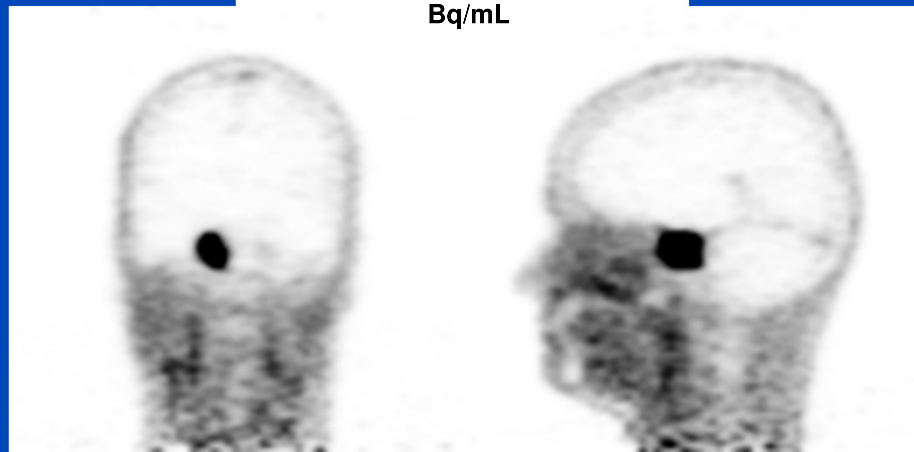

NAC vs. AC
Ga68 - Measured Data (2)

Non Attenuation-corrected Image (NAC)

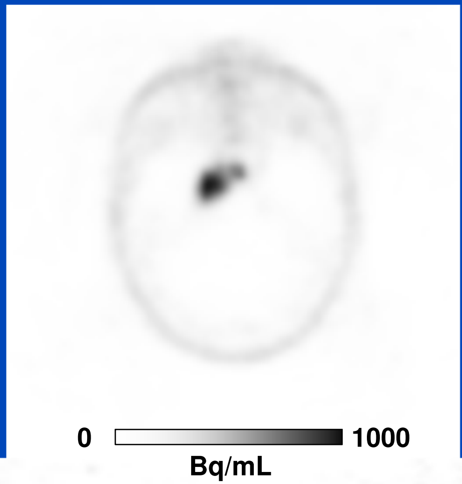

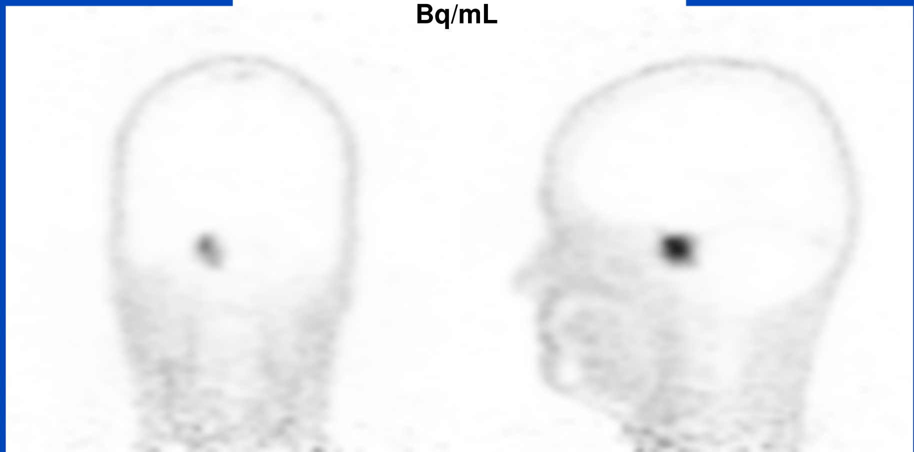

Half-life:
$T_{1/2}$ = 68 min

Attenuation-corrected Images (AC)

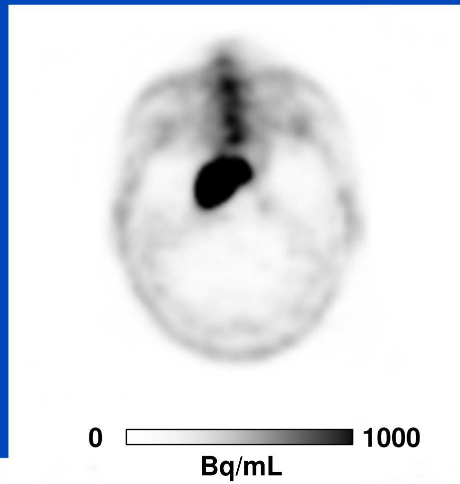

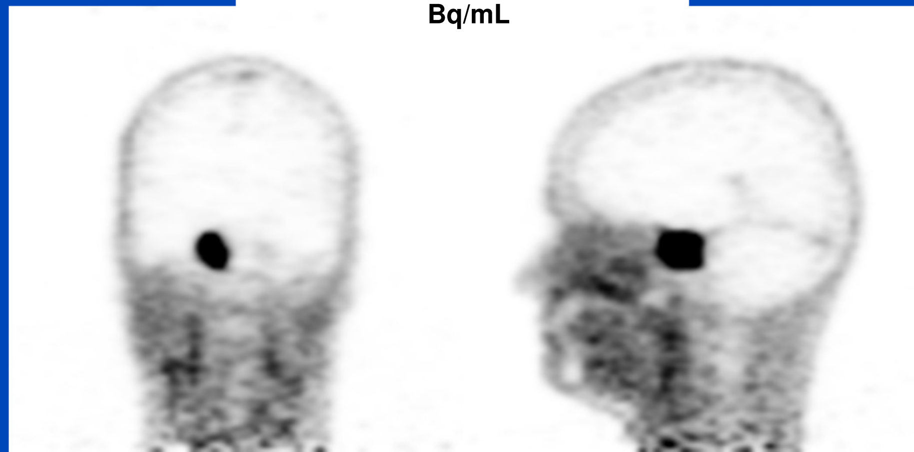

AC for Stand-alone PET

- **Transmission scan using known activities.**
- **Blank scan (without patient).**
- **Compare measured intensities.**
- **Attenuation correction factors for each LOR j:**

$$a_j = \frac{I_{0,j}}{I_j}$$

blank scan intensity

transmission scan intensity

Transmission Scan

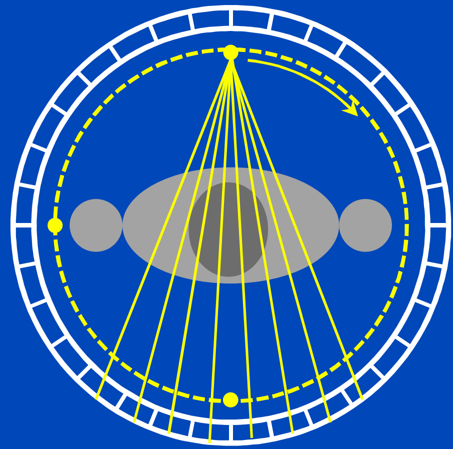

Blank Scan

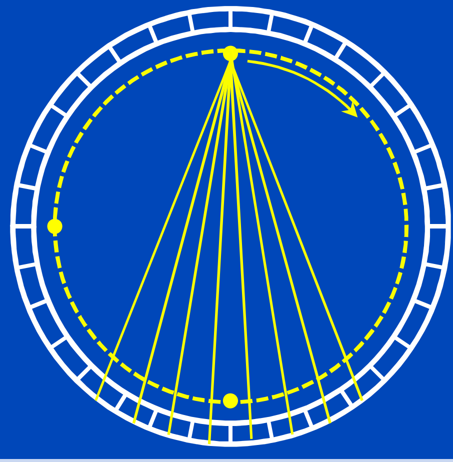

dkfz.

AC for PET/CT

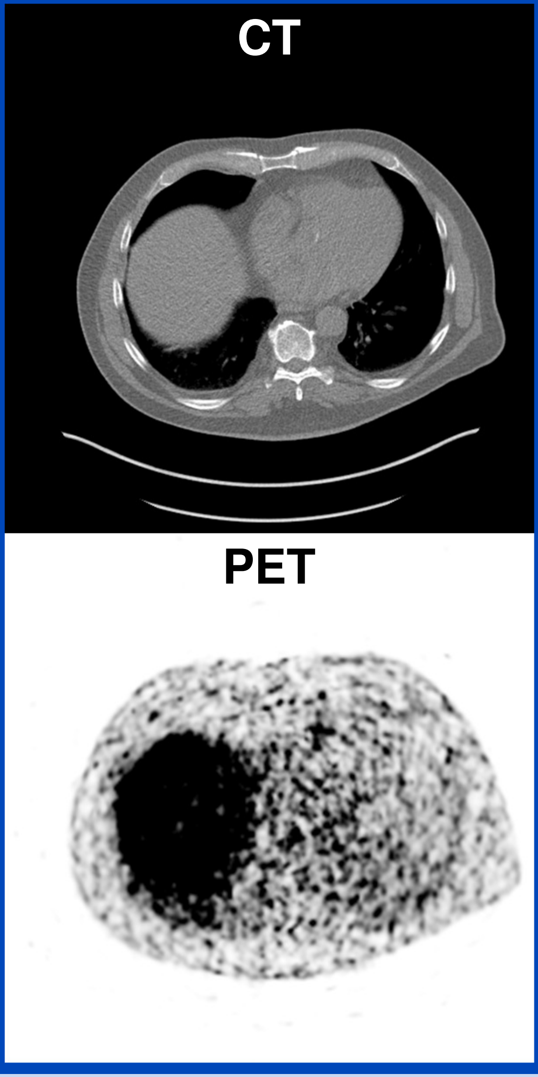

- **Attenuation map is obtained by bilinear scaling using the CT image[1].**

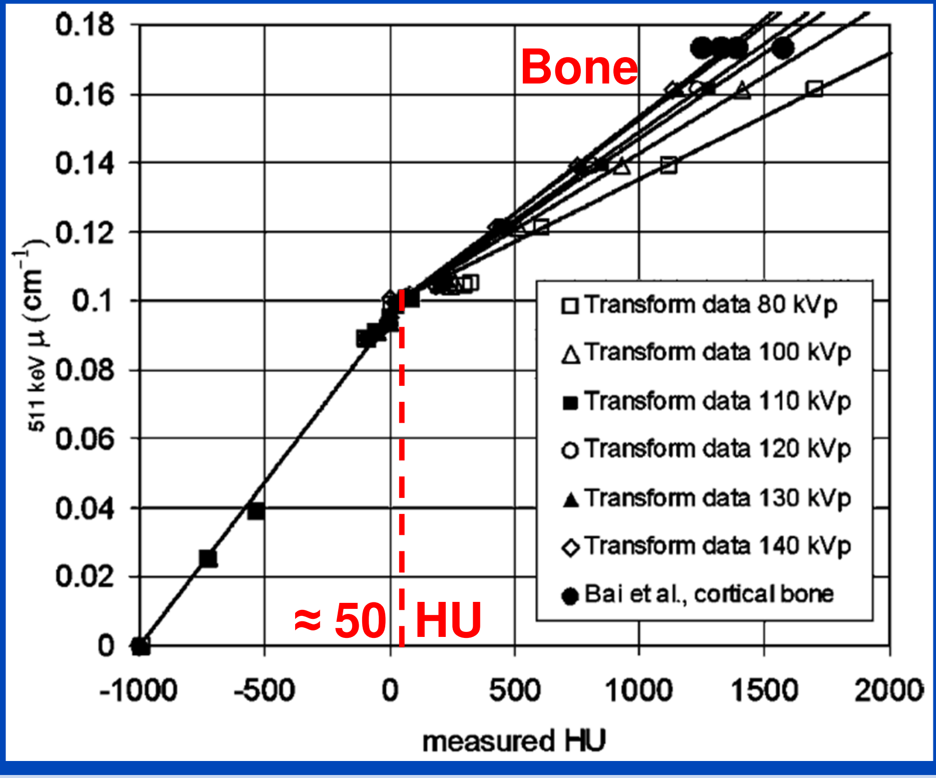

[1] J. P. J. Carney, D. W. Townsend, V. Rappoport, and B. Bendriem, "Method for transforming CT images for attenuation correction in PET/CT imaging," *Med. Phys.*, vol. 33, no. 4, pp. 976–83, 2006.

AC for PET/MR

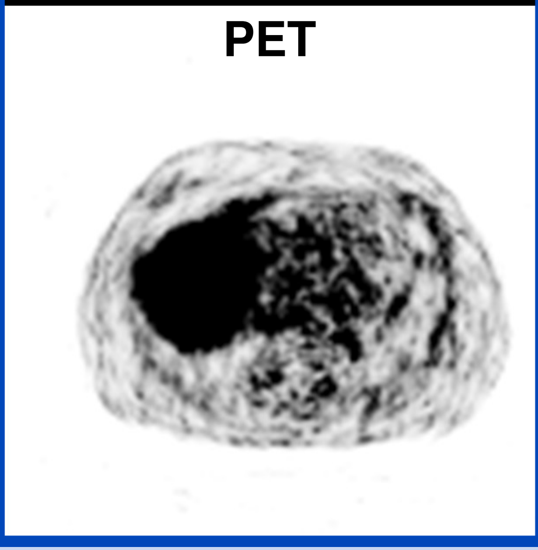

MR images obtained using two-point Dixon VIBE sequence

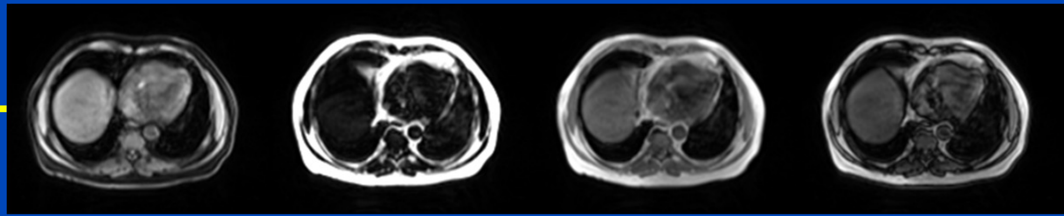

- MR images are used to segment different tissue classes (e.g., air, lung, fat, soft tissue).
- Appropriate attenuation values are assigned for each tissue class.
- Dedicated

dkfz.

Analytical 3D PET Reconstruction

- Direct analytic reconstruction of the 3D data
  - 3D Filtered backprojection (FBP)
  - 3D reprojection algorithm (3DRP)
- Rebinning methods to convert the 3D data into sets of 2D data (subsequently: 2D reconstruction)
  - Single Slice Rebinning (SSRB)
  - Fourier Rebinning (FORE)

- Quantitative corrections of the projection data necessary before reconstruction!

LOR Parametrization in 3D

- **LOR in 3D is parametrized by two transversal and two longitudinal variables.:**

$$p = p(\vartheta, \xi, \bar{z}, \delta) = p(\vartheta + \pi, -\xi, \bar{z}, -\delta)$$

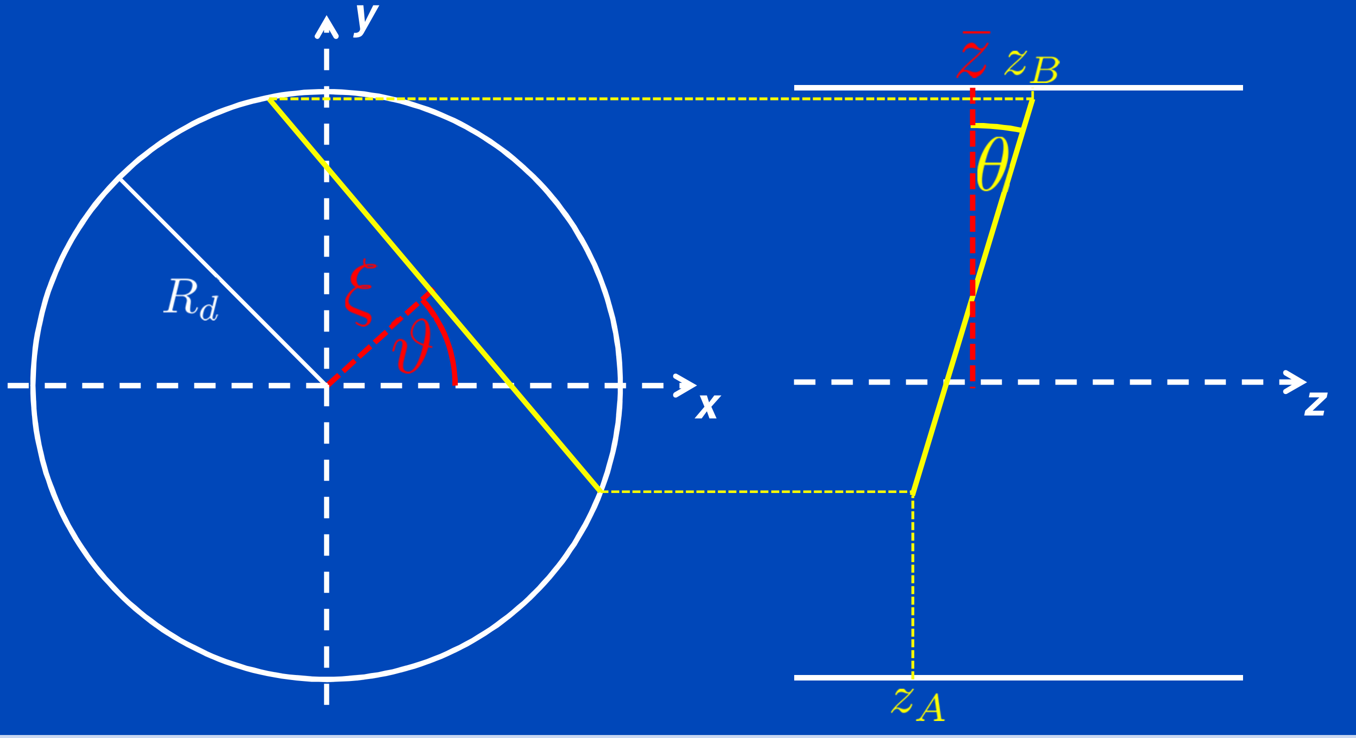

$$\bar{z} = \frac{z_A + z_B}{2}$$

$$\Delta = z_A - z_B$$

$$\delta = \tan\theta = \frac{\Delta}{2\sqrt{R_d^2 - \xi^2}}$$

dkfz.

3D Data Organization

- **2D parallel "sinograms"**
  - Group all LORs for given (ϑ, θ)

$$p(\vartheta, \xi, \cdot, \cdot)$$

  - Used for direct reconstruction (FBP, 3DRP)

- **Oblique sinograms**
  - Group all LORs for given $(\bar{z}, \delta)$

$$p(\cdot, \cdot, \bar{z}, \delta)$$

  - Used for rebinning approaches (SSRB, FORE)

$$\bar{z} = \frac{z_A + z_B}{2} \qquad \Delta = z_A - z_B$$

$$\delta = \tan\theta = \frac{\Delta}{2\sqrt{R_d^2 - \xi^2}}$$

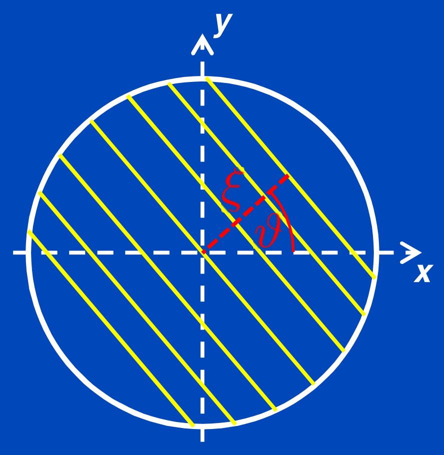

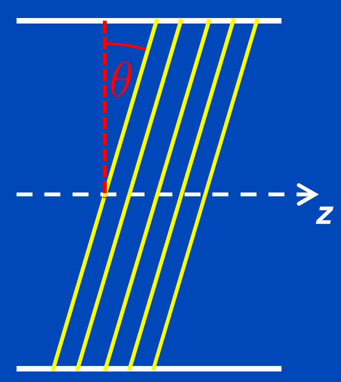

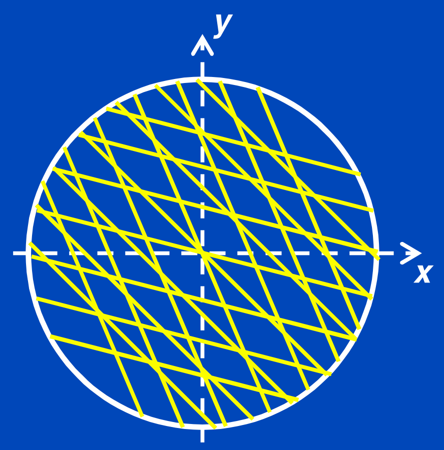

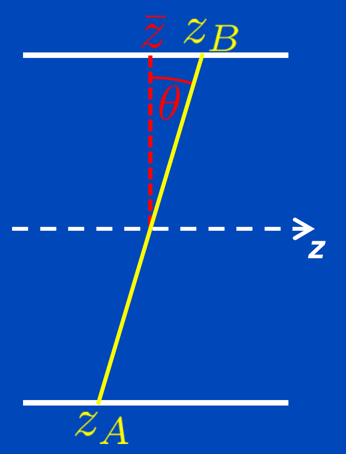

3D Filtered Backprojection (FBP)

- **Projections**

$$p(\boldsymbol{n}, \boldsymbol{\xi}) = \int dt\, \lambda(\boldsymbol{\xi} + t\boldsymbol{n})$$

$$\boldsymbol{n} = \begin{pmatrix} -\sin\vartheta\cos\theta \\ \cos\vartheta\cos\theta \\ \sin\theta \end{pmatrix}$$

$$\boldsymbol{\xi} \in \boldsymbol{n}^{\perp}$$

- **3D FBP**

$$\lambda(\boldsymbol{r}) = \int d\boldsymbol{n}\, p(\boldsymbol{n}, \boldsymbol{\xi}) * k(\boldsymbol{n}, \boldsymbol{\xi})|_{\boldsymbol{\xi} = \boldsymbol{r} - (\boldsymbol{r}\cdot\boldsymbol{n})\boldsymbol{n}}$$

Activity distribution

Convolution kernel (filter)

- **Only possible for non-truncated projections!**

3D Reprojection Algorithm (3DRP)[1]

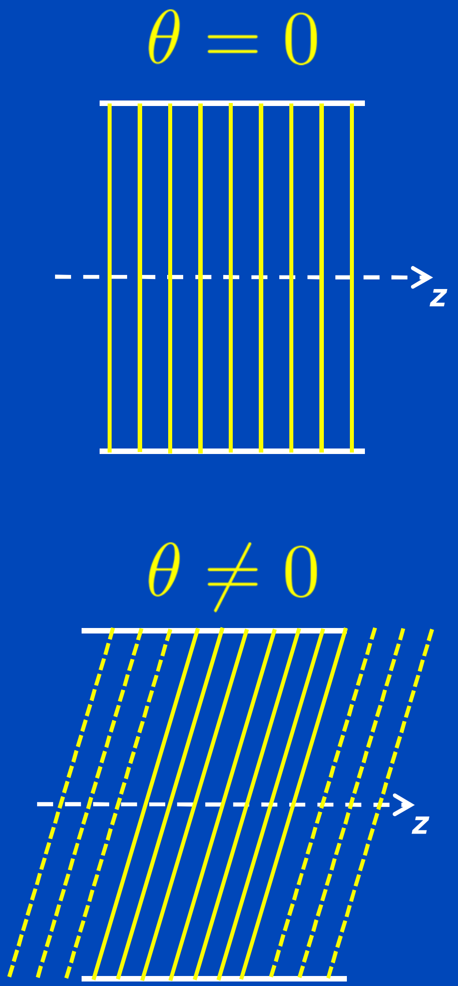

- **Measured projections are truncated for all longitudinal angles $\theta \neq 0$.**
- **3DRP is the standard analytic reconstruction in PET.**
- **Steps**
  1) **Use 2D FBP to reconstruct preliminary image from the $\theta = 0$ projection data.**
  2) **Forward project preliminary image along missing LORs ($\theta \neq 0$).**
  3) **Reconstruct measured and forward projected data using 3D FBP.**

[1] P. E. Kinahan and J. G. Rogers, "Analytic 3D image reconstruction using all detected events ," *IEEE Trans. Nucl. Sci.*, vol. 36, no. 1, pp. 964–968, 1989.

dkfz.

Rebinning in PET

- Estimate stack of 2D sinograms from available 3D data by longitudinal resorting or averaging.
- Use 2D methods to reconstruct the rebinned projections.
- Similar sensitivity as 3D methods but much faster.
- Approximate.

Single-slice Rebinning Algorithm (SSRB)[1]

- Direct rebinning in projection domain

$$p_{\mathrm{ssrb}}(\vartheta, \xi, z) = \frac{1}{2\delta_{\max}} \int_{-\delta_{\max}}^{\delta_{\max}} d\delta\, p(\vartheta, \xi, \bar{z}, \delta)$$

max. longitudinal aperture

- SSRB is quite accurate if
  - max. longitudinal aperture $\theta_{\max}$ is small.
  - activity is concentrated along the longitudinal scanner axis.
  - activity is invariant in longitudinal direction.

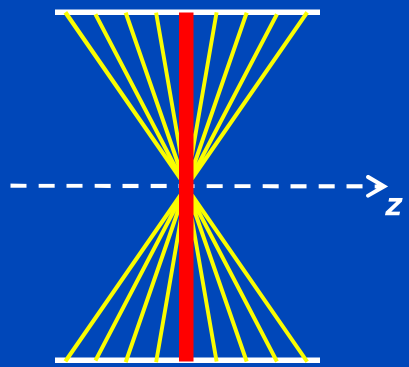

[1] M. E. Daube-Witherspoon and G. Muehllehner, "Treatment of axial data in three-dimensional PET.," *J. Nucl. Med.*, vol. 28, no. 11, pp. 1717–24, Nov. 1987.

Fourier Rebinning Algorithm (FORE)[1]

- **Rebinning in Fourier domain**
  1) 2D FT of oblique projection data

$$P(\nu, k, \bar{z}, \delta) = Fp(\vartheta, \xi, \bar{z}, \delta)$$

  2) Average and normalize

$$P_{\text{fore}}(\nu, k, \bar{z}, \delta = 0) = \frac{1}{2\delta_{\max}} \int_{-\delta_{\max}}^{\delta_{\max}} d\delta P(\nu, k, \bar{z} + \delta\frac{\nu}{k}, \delta)$$

  3) 2D inverse FT to obtain rebinned projections for every *z*-slice

$$p_{\text{fore}}(\vartheta, \xi, z) = F^{-1} P_{\text{fore}}$$

[1] M. Defrise, P. E. Kinahan, D. W. Townsend, C. Michel, M. Sibomana, and D. F. Newport, "Exact and approximate rebinning algorithms for 3-D PET data.," *IEEE Trans. Med. Imaging*, vol. 16, no. 2, pp. 145–58, Apr. 1997.

Morgen Vormittag:
Iterative Bildrekonstruktion

gated gridding | **HDTV** | **MoCo** MVF from cMoCo | **MoCo-HDTV** MVF from cMoCo

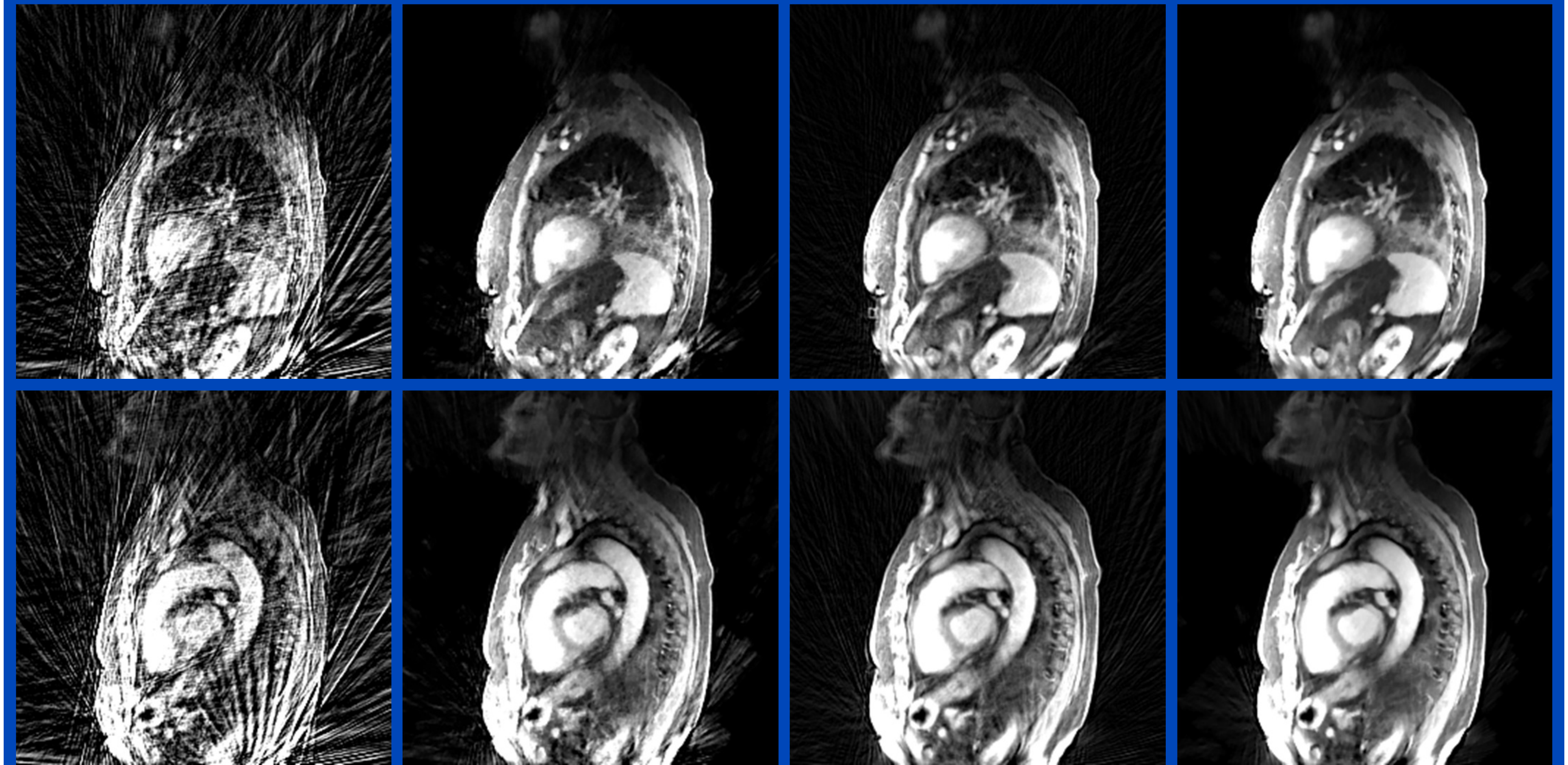

480 radial spokes per slice, 20 overlapping phases, acquisition time: 69 s

Thank You!

This presentation will soon be available at www.dkfz.de/ct.

Parts of the reconstruction software were provided by RayConStruct® GmbH, Nürnberg, Germany.